Approximations and simulations for the construction of templates

Alessandra Buonanno
Department of Physics, University of Maryland

"Interplay between Data Analysis and Numerical Relativity"

Motivation/Outline

- **Goal: build analytical templates for inspiral, merger and ringdown to be used to detect GWs and extract binary parameters**

- **How to reach this goal? Several tools are available:**

– **Accurate PN-expanded results for the inspiral phase**

– **PN-resummed methods beyond the inspiral phase (effective-one-body/Padé, etc.)**

– **Non-perturbative information contained in several numerical-relativity simulations**

– **Insights from black hole perturbation theory and test-mass limit**

– **Qualitative understanding of the** *basic physical features* **determining the waveforms**

– **Comparison between analytical and numerical relativity results**

- **Where we stand in this programme. What still needs to be done**

Why we need *analytical* templates?

- **The high computational cost of running numerical simulations makes it difficult to generate sufficiently long and accurate waveforms that cover the parameter space of astrophysical interest**

- **By *analytical* templates we mean also templates obtained by solving ordinary differential equations. This is computationally faster than running a numerical simulation**

Why we need templates to search coherently for inspiral-merger-ringdown signals

[Pan, AB, Pretorius & NASA-Goddard 07]

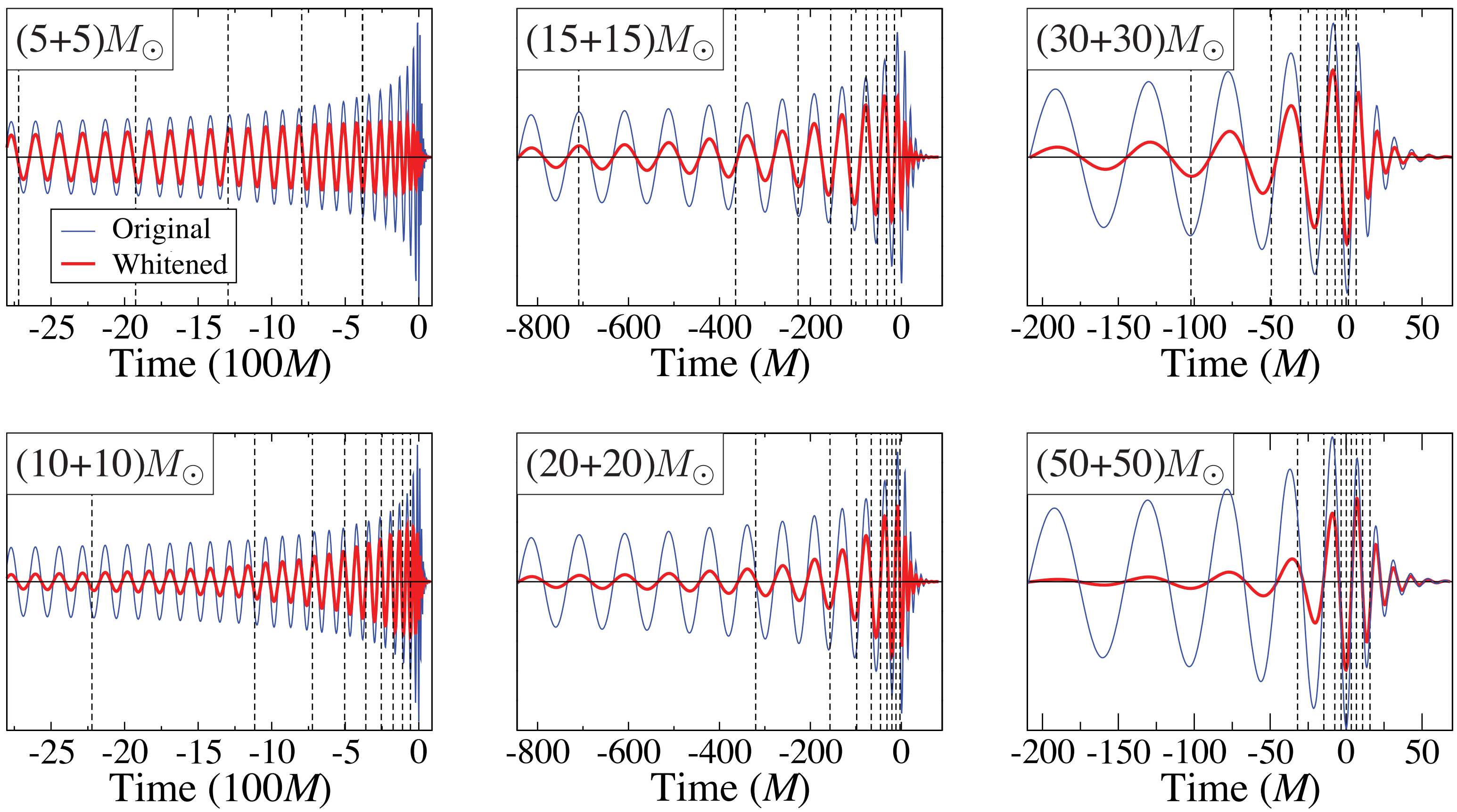

Modeling the long inspiral phase using PN theory

[Blanchet, Damour, Iyer, Schaefer, Jaranowski, Faye; Will, Wiseman, Kidder, ...]

- **In general relativity radiation-reaction effects appear at order $\sim v^5/c^5$ beyond the Newtonian force law**

$$m\,\frac{d\mathbf{v}}{dt} = \mathbf{F}_{\rm Newt} + \cdots + \left(\frac{v}{c}\right)^5 \mathbf{F}_{\rm RR}$$

- **Throughout the inspiral $T_{\rm RR} \gg T_{\rm orb} \Rightarrow$ natural** *adiabatic parameter*

$$\frac{\dot{\omega}}{\omega^2} = \mathcal{O}\left[\left(\frac{v}{c}\right)^5\right]$$

- **PN expansion: formal expansion in $1/c$ when $c \to +\infty$**

- **For compact bodies, such as neutron stars and black holes,**

$$\frac{v^2}{c^2} \sim \frac{Gm}{c^2 r} \sim \frac{R_S}{r} \ll 1$$

PN-expanded-approximants for the inspiral phase in the adiabatic approximation

- **Waveform in the *restricted* approximation**

$$h(t) \propto \ddot{Q} \propto \frac{v^2}{c^2} \cos 2\varphi \propto \left(\frac{GM\,\omega}{c^3}\right)^{2/3} \cos 2\varphi$$

- **Energy-balance equation:** $\frac{dE(v)}{dt} = -F(v)$

$E(v) \to$ center-of-mass energy $F(v) \to$ gravitational-wave energy flux

$E(v)$ **and** $F(v)$ **known as a PN expansion in** $v/c = (GM\omega/c^3)^{1/3}$

$$\Rightarrow \dot{\omega} = -\frac{F(\omega)}{[dE(\omega)/d\omega]} \quad \Rightarrow \quad \varphi_{\rm GW}(t) = 2\varphi(t) = 1/\pi \int \omega\, dt$$

PN-expanded-approximants for the inspiral phase in time domain

Equal-mass binary; $+$ polarization along the z-axis

$$h_+^{(z)}(t) \quad \propto \quad \omega^{2/3} \left\{ \cos 2\varphi \left[-2 + \frac{17}{4}\omega^{2/3} - 4\pi\omega + \frac{15917}{2880}\omega^{4/3} + 9\pi\omega^{5/3} \right] + \sin 2\varphi \left[-\frac{24}{3} \ln\left(\frac{\omega}{\omega_0}\right)\omega + \left[\frac{59}{5} + \frac{54}{3} \ln\left(\frac{\omega}{\omega_0}\right) \right] \omega^{5/3} \right] \right\}$$

Higher-order amplitude corrections are available through 2.5 PN (3PN for some modes) for non-spinning BHs and 1.5PN for spinning BHs

[Blanchet et al. 96; Arun et al. 04; Kidder et al. 07; Kidder 07; Will & Wiseman 96; Kidder 95]

PN-expanded-approximants for the inspiral phase in Fourier domain

$$\tilde{h}_{\rm SPA}(f) = \mathcal{A}_{\rm SPA}(f)\, e^{i\psi_{\rm SPA}(f)} \qquad \mathcal{A}_{\rm SPA}(f) \propto f^{-7/6}$$

$$\begin{aligned}\psi_{\rm SPA}(f) &= 2\pi f t_c - \varphi_c - \pi/4 + \frac{3}{128}(\pi\mathcal{M}f)^{-5/3}\,\{1+ \\ &+ \left(\frac{3715}{756} + \frac{55}{9}\eta\right)\eta^{-2/5}(\pi\mathcal{M}f)^{2/3} - 16\pi\,\eta^{-3/5}(\pi\mathcal{M}f) + 4\beta\,\eta^{-3/5}(\pi\mathcal{M}f) \\ &+ \left(\frac{15293365}{508032} + \frac{27145}{504}\eta + \frac{3085}{72}\eta^2\right)\eta^{-4/5}(\pi\mathcal{M}f)^{4/3} - 10\sigma\,\eta^{-4/5}(\pi\mathcal{M}f)^{4/3} + \dots\Big\}\end{aligned}$$

$$\beta = \frac{1}{12}\sum_{i=1}^{2}\chi_i\left[113\frac{m_i^2}{M^2} + 75\eta\right]\hat{\boldsymbol{L}}\cdot\hat{\boldsymbol{S}}_i\,, \qquad \sigma = \frac{\eta}{48}\chi_1\chi_2\left(-27\hat{\boldsymbol{S}}_1\cdot\hat{\boldsymbol{S}}_2 + 721\hat{\boldsymbol{L}}\cdot\hat{\boldsymbol{S}}_1\hat{\boldsymbol{L}}\cdot\hat{\boldsymbol{S}}_2\right)$$

For higher-order PN corrections in the SPA phase see `Arun et al. 04; Arun and Ochsner (in prep.)`

Stationary phase approximation

$$\tilde{h}(f) = \frac{1}{2} \int_{-\infty}^{+\infty} dt\, A(t)\, \left[e^{2\pi i f t + i \varphi_{\rm GW}(t)} + e^{2\pi i f t - i \varphi_{\rm GW}(t)} \right]$$

Dominant contribution from the vicinity of the *stationary* **points in the phase**

Assuming $f > 0$ **and posing** $\psi(t) \equiv 2\pi\, f\, t - \varphi_{\rm GW}$

Imposing $\left(\frac{d\psi}{dt}\right)_{t_f} = 0 \;\Rightarrow\; \left(\frac{d\varphi_{\rm GW}}{dt}\right)_{t_f} = 2\pi\, f = 2\pi F(t_f)$

Expanding the phase: $\psi(t_f) = 2\pi\, f\, t_f - \varphi_{\rm GW}(t_f) - \pi\, \dot{F}(t_f)\,(t - t_f)^2$

$$\tilde{h}_{\rm SPA}(f) = \frac{1}{2} \frac{A(t_f)}{\sqrt{\dot{F}(t_f)}}\, e^{i(2\pi\, f\, t_f - \varphi_{\rm GW}(t_f)) - i\pi/4}$$

For higher-order PN corrections in the SPA amplitude see `Van den Broeck et al. 07; Arun and Ochsner (in prep.)`

Effective-one-body and Padé resummation

[AB & Damour 99]

- **Resum so that *known* test mass limit results are recovered**

- **Resum the PN expansion assuming that the equal-mass limit is a η-deformation of the test-mass limit**

$$\eta = m_1\, m_2/M^2$$

$$0 \leq \eta \leq 1/4$$

- **Padé resummation of the energy flux F**

[Damour, Iyer & Sathyaprakash 98]

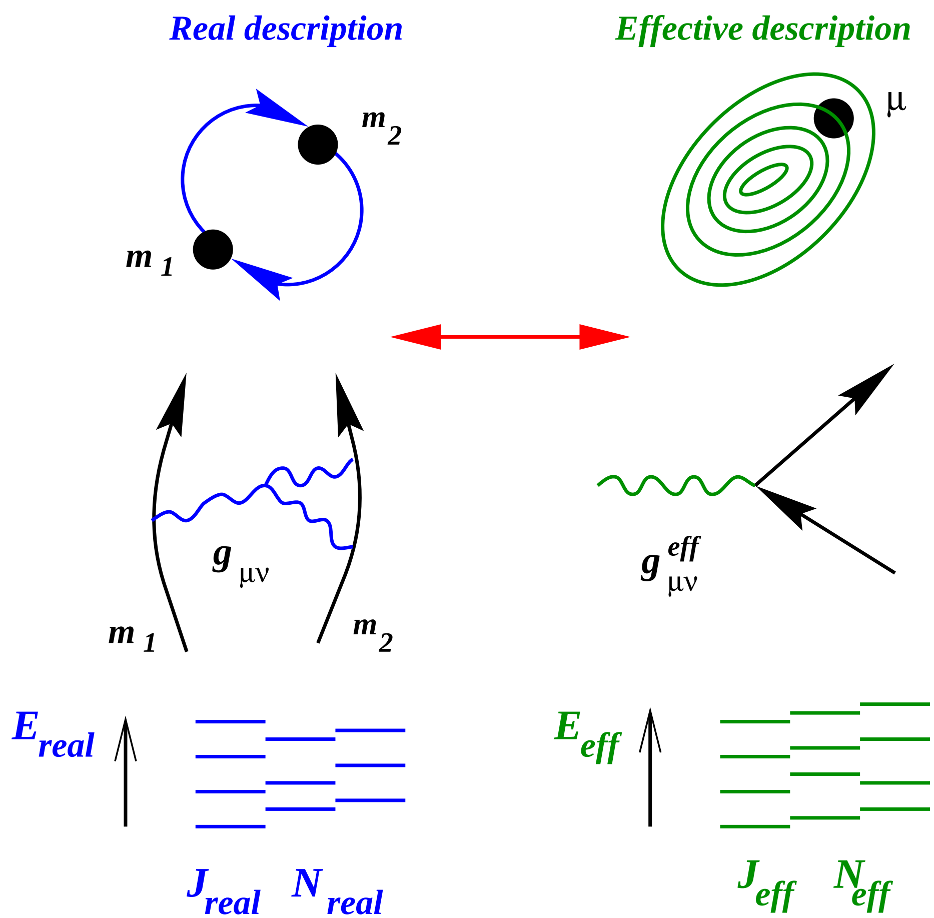

$$E_{\rm real}(\mathcal{N}_{\rm real}, J_{\rm real}) = f\,[E_{\rm eff}(\mathcal{N}_{\rm eff}, J_{\rm eff})]$$

Key ideas to build the effective-one-body approach

[AB & Damour 99]

- **PN-expanded Hamiltonian in the center-of-mass:**

$$H(\boldsymbol{Q},\boldsymbol{P}) = H_{\rm Newt}(\boldsymbol{Q},\boldsymbol{P}) + \frac{1}{c^2}\,H_{\rm 1PN}(\boldsymbol{Q},\boldsymbol{P}) + \frac{1}{c^4}\,H_{\rm 2PN}(\boldsymbol{Q},\boldsymbol{P})$$

At the Newtonian approximation $H_{\rm Newt}(\boldsymbol{Q},\boldsymbol{P})$ describes a test-particle of mass μ orbiting around an *external mass* GM

- **The EOB approach is a general relativistic generalization of this fact:**
  Find an *effective (or external) spacetime geometry* $g_{\mu\nu}^{\rm eff}(x^\alpha; GM)$ **such that the geodesics dynamics of a "test-particle" of mass μ moving in $g_{\mu\nu}^{\rm eff}(x^\alpha; GM)$ is** *equivalent* **(when expanded in powers of $1/c^2$) to the original PN-expanded dynamics**

- **The equivalence between the two dynamics can be thought as the equivalence between the (quantized) energy spectra**

$$E_{\rm real}(\mathcal{N}_{\rm real}, J_{\rm real}) = f\,[E_{\rm eff}(\mathcal{N}_{\rm eff}, J_{\rm eff})]$$

EOB approach: resummed Hamiltonian (non-spinning black holes)

[AB & Damour 99; Damour, Jaranowski & Schaefer 00]

"Real" description

$$\mathcal{H}_{\rm real}(\boldsymbol{Q},\boldsymbol{P}) \sim M\left\{1+\eta\left[\frac{\boldsymbol{P}^2}{2}+\frac{M}{Q}\right]+c_4\,\boldsymbol{P}^4+\cdots\right\}$$

"Effective" description

$$\mathcal{H}^{\eta}_{\rm eff}(\boldsymbol{q},\boldsymbol{p}) = \sqrt{A_\eta(q)\,\left[1+\boldsymbol{p}^2+\left(\frac{A_\eta(q)}{D_\eta(q)}-1\right)\,(\boldsymbol{n}\cdot\boldsymbol{p})^2+\mathcal{T}_4(\boldsymbol{p})\right]}$$

$$\boxed{\mathcal{H}^{\rm impr}_{\rm real}(\boldsymbol{Q},\boldsymbol{P}) = \sqrt{1+2\eta\,\left(\mathcal{H}^{\eta}_{\rm eff}(\boldsymbol{q},\boldsymbol{p})-1\right)}}$$

$$ds^2_{\rm eff} = -A_\eta(q)\,dt^2+\frac{D_\eta(q)}{A_\eta(r)}\,dq^2+q^2\,d\Omega^2$$

- **All dynamics condensed in $A_\eta(q)$ and $D_\eta(q)$**
- $g^{\rm eff}_{00}$ **which encodes the energetics for circular orbits is rather** *simple*

$$A_\eta(q) = 1-\frac{2}{q}+\frac{2\eta}{q^3}+\left(\frac{94}{3}-\frac{41}{32}\pi^2\right)\frac{\eta}{q^4}$$

- **To ensure physical features, $A_\eta(q)$ can be replaced by a suitable Padé approximant**

EOB approach with spins

- **Mapping to a suitable Kerr-deformed spacetime** [Damour 01]

$$\mathcal{H}_{\rm eff}^{\rm Kerr}(\boldsymbol{q},\boldsymbol{p},\boldsymbol{S}_1,\boldsymbol{S}_2) = \beta_i\, p^i + \alpha\,\sqrt{1+\gamma^{ij}\,p_i\,p_j + \mathcal{T}_4(p_i)}$$

$$g^{00}_{\rm eff} = -\frac{1}{\alpha^2} \quad g^{0i}_{\rm eff} = -\frac{\beta^i}{\alpha^2} \propto (\boldsymbol{S}\times\boldsymbol{q})^i \quad g^{ij}_{\rm eff} = \gamma^{ij} - \frac{\beta^i\,\beta^j}{\alpha^2}$$

$$\mathcal{H}_{\rm real}(\boldsymbol{Q},\boldsymbol{P},\boldsymbol{S}_1,\boldsymbol{S}_2) = \sqrt{1+2\eta\,\left(\mathcal{H}_{\rm eff}^{\rm Kerr}(\boldsymbol{q},\boldsymbol{p},\boldsymbol{S}_1,\boldsymbol{S}_2)-1\right)}$$

- **Alternatively, spin effects can be added to the non-spinning EOB Schwarzschild-deformed Hamiltonian** [AB, Chen & Damour 05]

$$\mathcal{H}_{\rm real}(\boldsymbol{Q},\boldsymbol{P},\boldsymbol{S}_1,\boldsymbol{S}_2) = \mathcal{H}_{\rm real}^{\rm Schw}(\boldsymbol{q},\boldsymbol{p}) + \mathcal{H}_{\rm SO}(\boldsymbol{q},\boldsymbol{p},\boldsymbol{S}_1,\boldsymbol{S}_2) + \mathcal{H}_{\rm SS}(\boldsymbol{q},\boldsymbol{p},\boldsymbol{S}_1,\boldsymbol{S}_2)$$

$$\mathcal{H}_{SO} = \frac{2\boldsymbol{S}_{\rm eff}\cdot\boldsymbol{L}}{q^3}, \quad \boldsymbol{S}_{\rm eff} \equiv \left(1+\frac{3}{4}\frac{m_2}{m_1}\right)\boldsymbol{S}_1 + \left(1+\frac{3}{4}\frac{m_1}{m_2}\right)\boldsymbol{S}_2$$

EOB approach: incorporating radiation reaction effects

[AB & Damour 00; AB, Chen & Damour 05]

$$\frac{dq^i}{dt} = \frac{\partial \mathcal{H}^{\rm EOB}}{\partial p_i} \qquad \frac{dp_i}{dt} = -\frac{\partial \mathcal{H}^{\rm EOB}}{\partial q^i} + \mathcal{F}_i$$

$$\frac{d\mathbf{S}_1}{dt} = \frac{\partial \mathcal{H}^{\rm EOB}}{\partial \mathbf{S}_1} \times \mathbf{S}_1 \qquad \frac{d\mathbf{S}_2}{dt} = \frac{\partial \mathcal{H}^{\rm EOB}}{\partial \mathbf{S}_2} \times \mathbf{S}_2$$

- **Radiation-reaction force matches known rates of energy and angular momentum loss for quasi-adiabatic orbits**

- **Padé resummation of the GW flux**

[Damour, Sathyaprakash & Iyer 98; Porter & Sathyaprakash 04; AB, Chen & Damour 05]

$$\hat{F}(v;\eta) = \frac{1}{1-v/v_{\rm pole}}\, f(v;\eta) \Rightarrow P[f(v;\eta)] = P[(1-v/v_{\rm pole})\, \hat{F}(v;\eta)]$$

Taylor and Padé approximants to the GW energy flux

[Damour, Iyer & Sathyaprakash 97]

test mass limit

Taylor-approximant

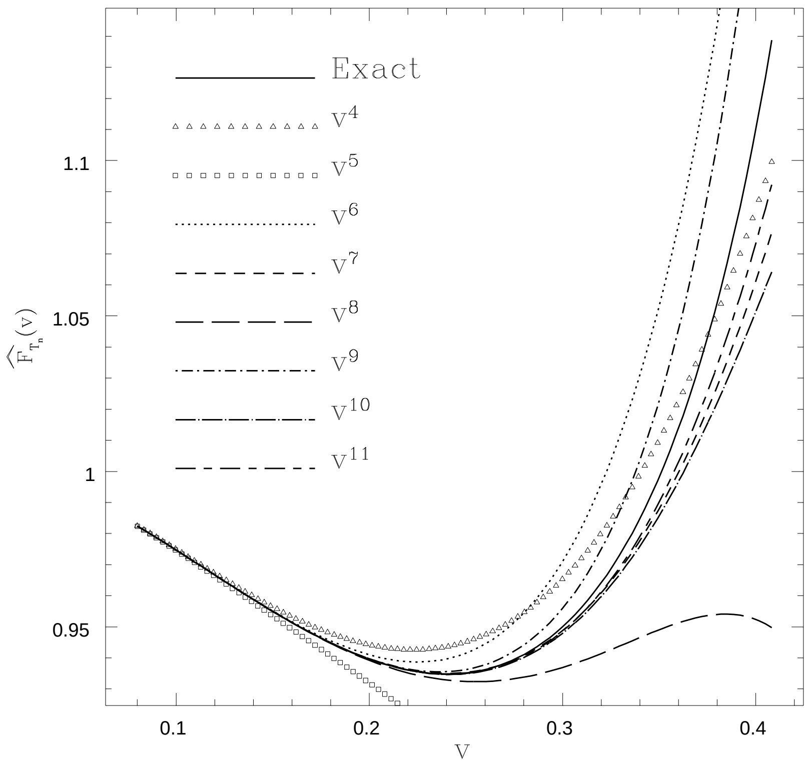

Padé-approximant

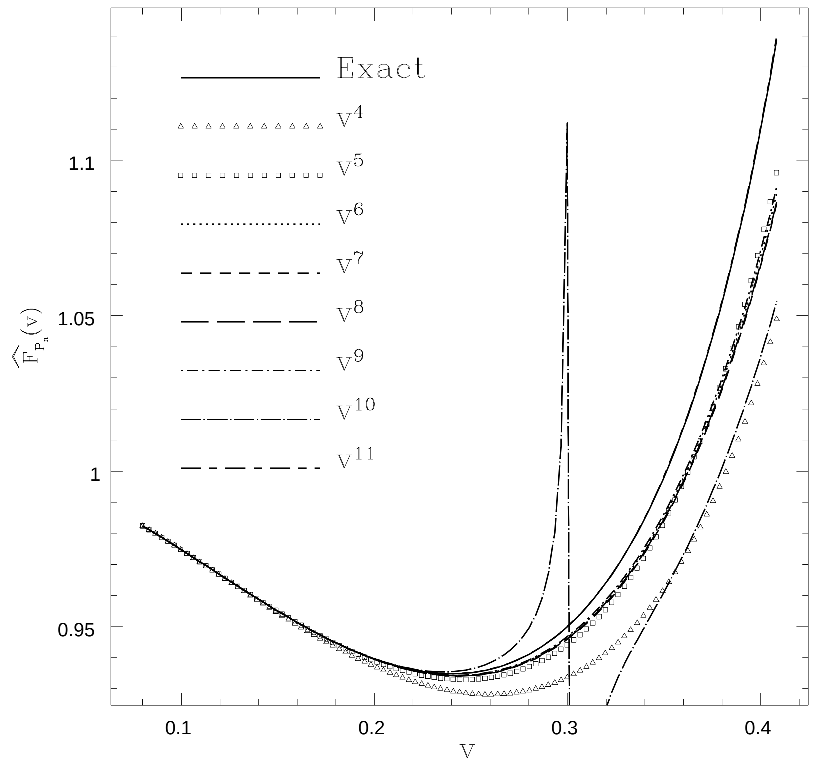

Key idea to incorporate merger-ringdown in the EOB approach

$$\frac{d^2}{dr_*^2} Z_l + (V_l - \omega^2)\, Z_l = \mathcal{S}_l$$

$Z_l \longrightarrow$ perturbation $\mathcal{S}_l \longrightarrow$ source

Outgoing field

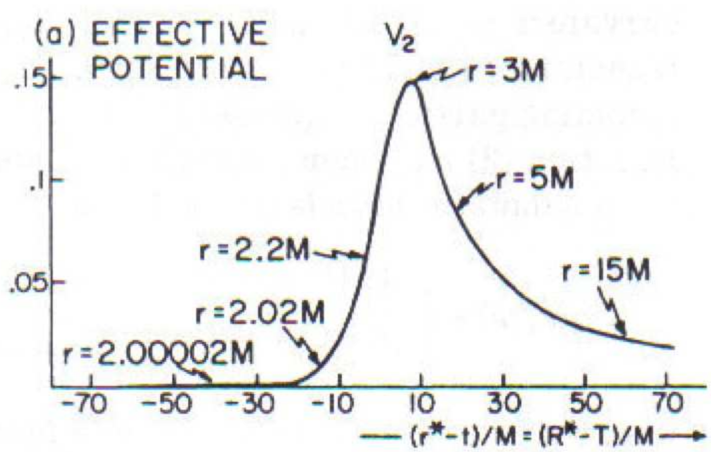

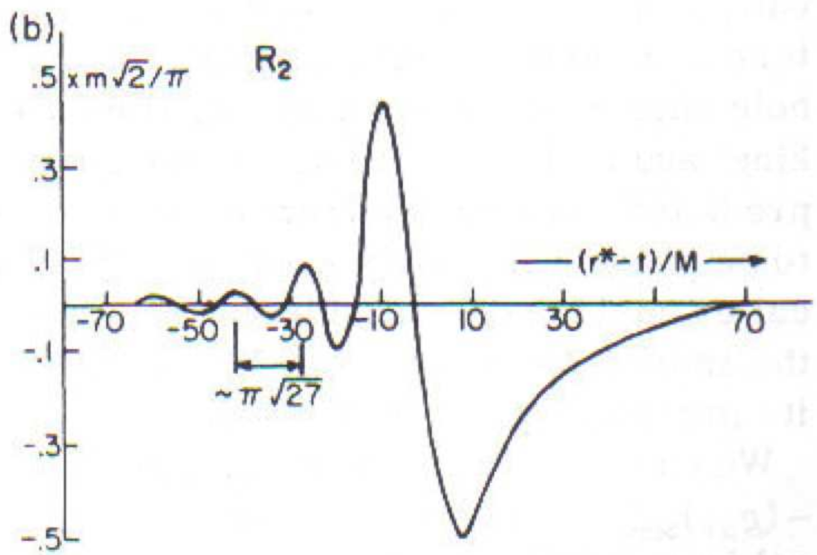

... part of the energy produced in the strong-burst region is stored in the resonant cavity of the geometry, and then slowly released in ringdown modes.

[Press 71; Davis, Ruffini, Press & Price 71; Davis, Ruffini & Tionmo 72]

Full waveform as predicted by the EOB-Padé model

- **The plunge (~ 1.5 GW cycles) is a smooth continuation of the inspiral phase**
- **The transition merger to ringdown was assumed** *very short*
- One single **QNM matched using** $M_{\rm BH} = E_{\rm LR} = 0.976\,M$, $a_{\rm BH} = \boldsymbol{J}_{\rm LR}/E^2_{\rm LR} = 0.77$

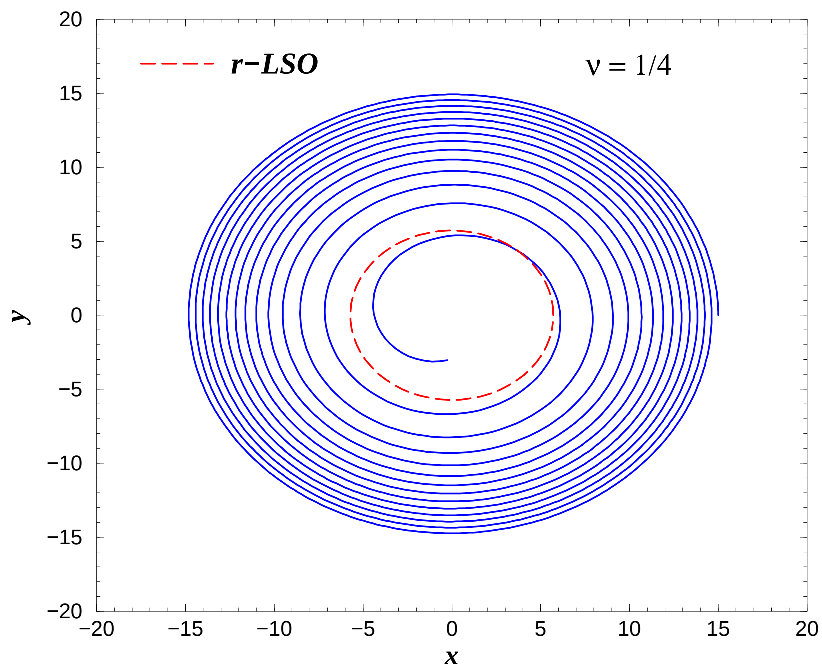

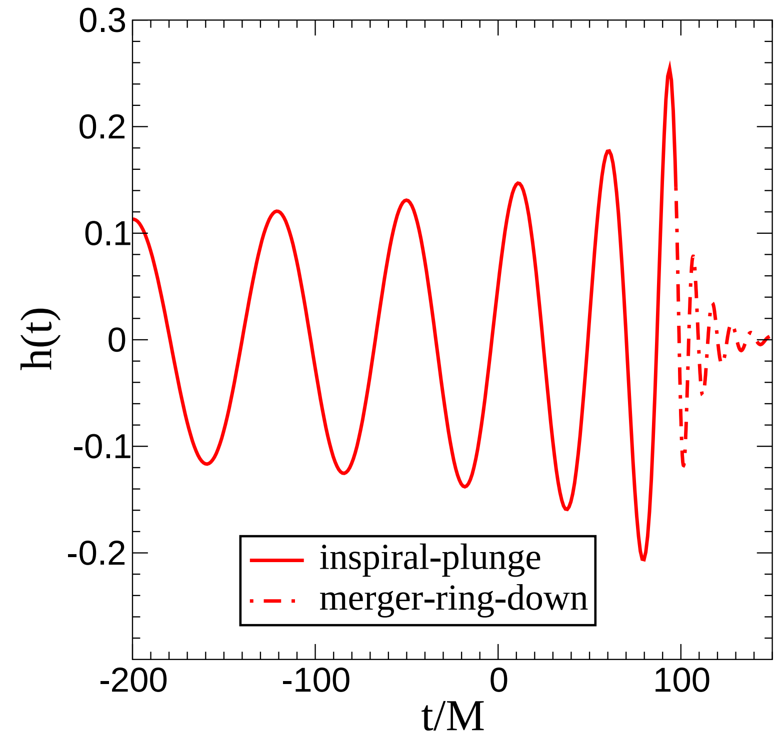

[AB & Damour 99, 00; Damour, Jaranowski & Schafer 00; Damour 01; AB, Chen & Damour 06]

Numerical simulations of equal-mass binary: *one* dominant frequency

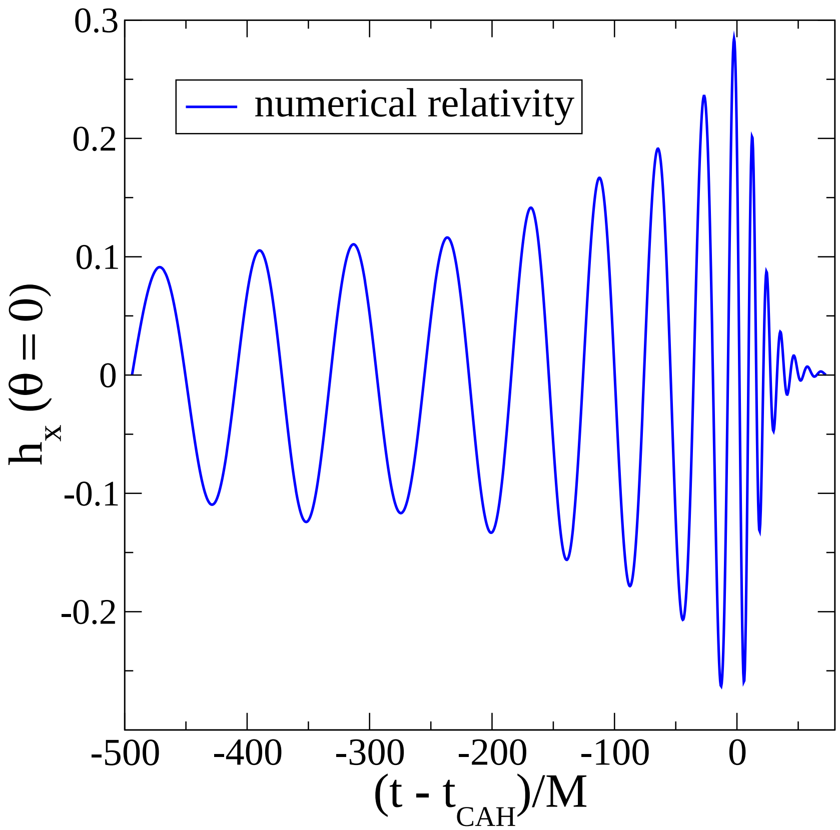

[AB, Cook & Pretorius 06]

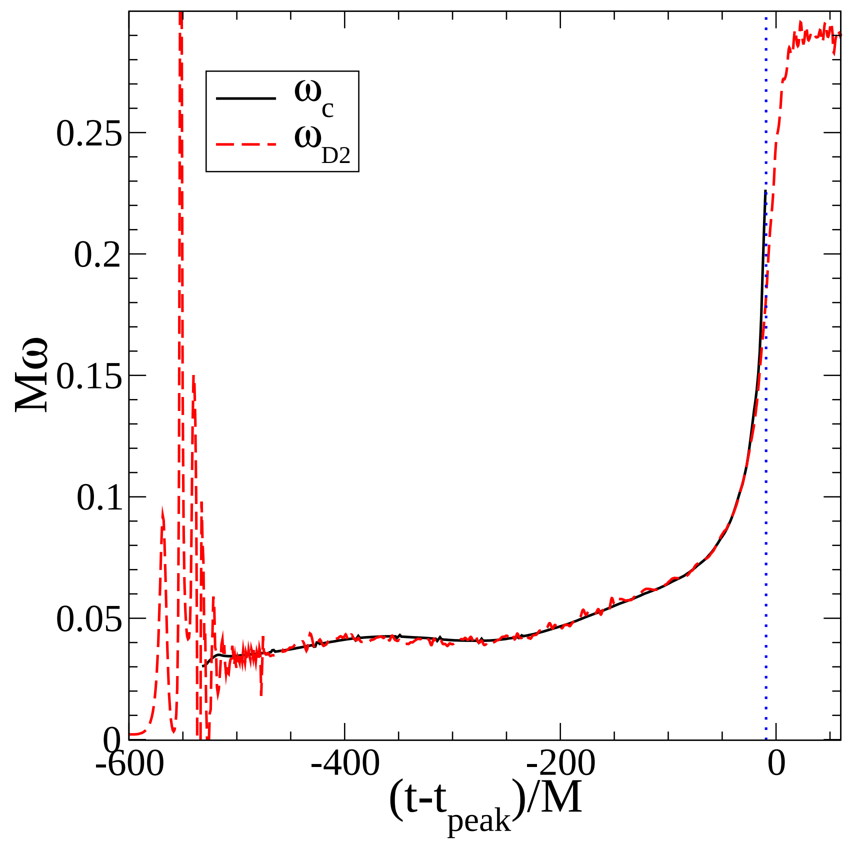

- $\omega_c \Leftarrow$ **from the coordinate separation**
- $\omega_{\rm D2} = -\frac{1}{2}{\rm Im}\left[\frac{\dot{C}_{22}}{C_{22}}\right] \Leftarrow$ **from the wave**

When the ringdown phase starts. Higher overtones.

[AB, Cook & Pretorius 06; see also Berti et al. 07]

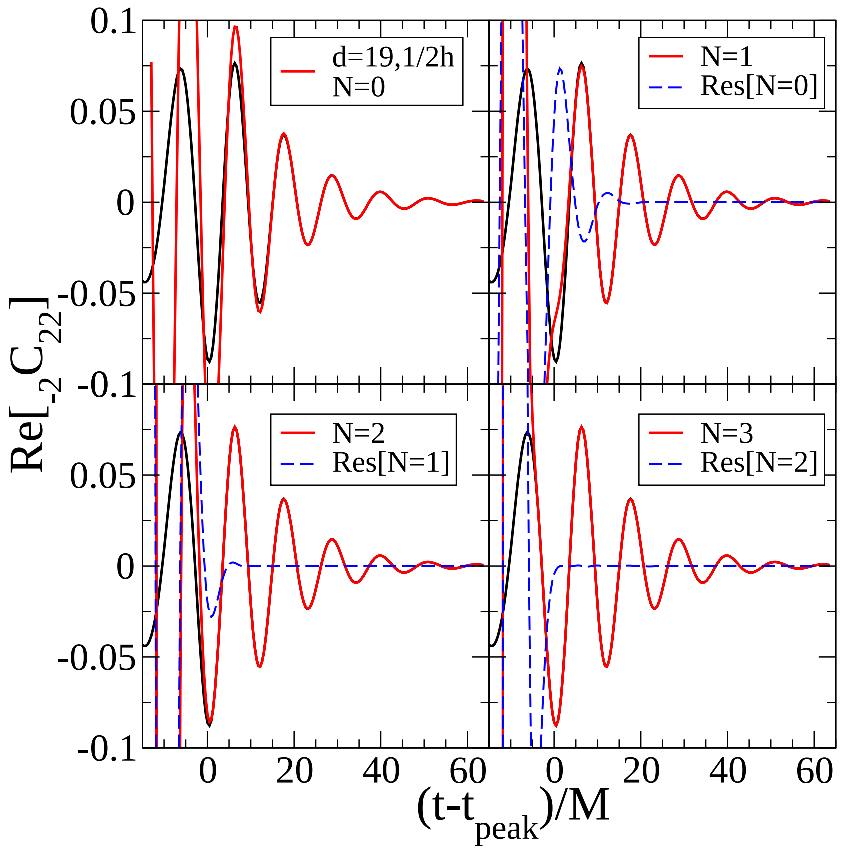

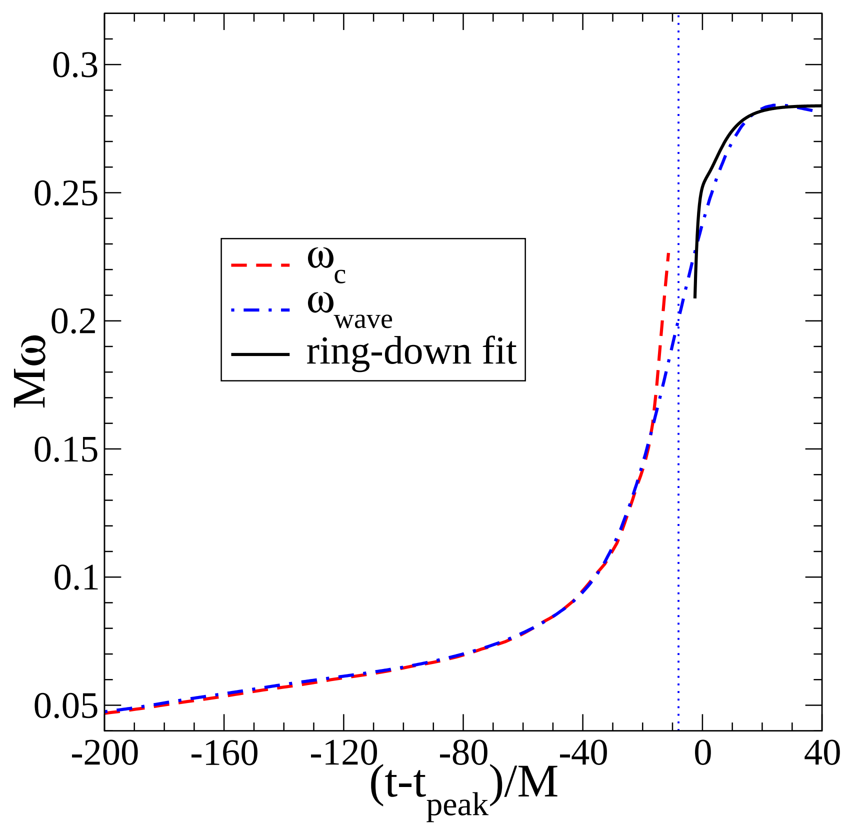

The (plunge and) merger

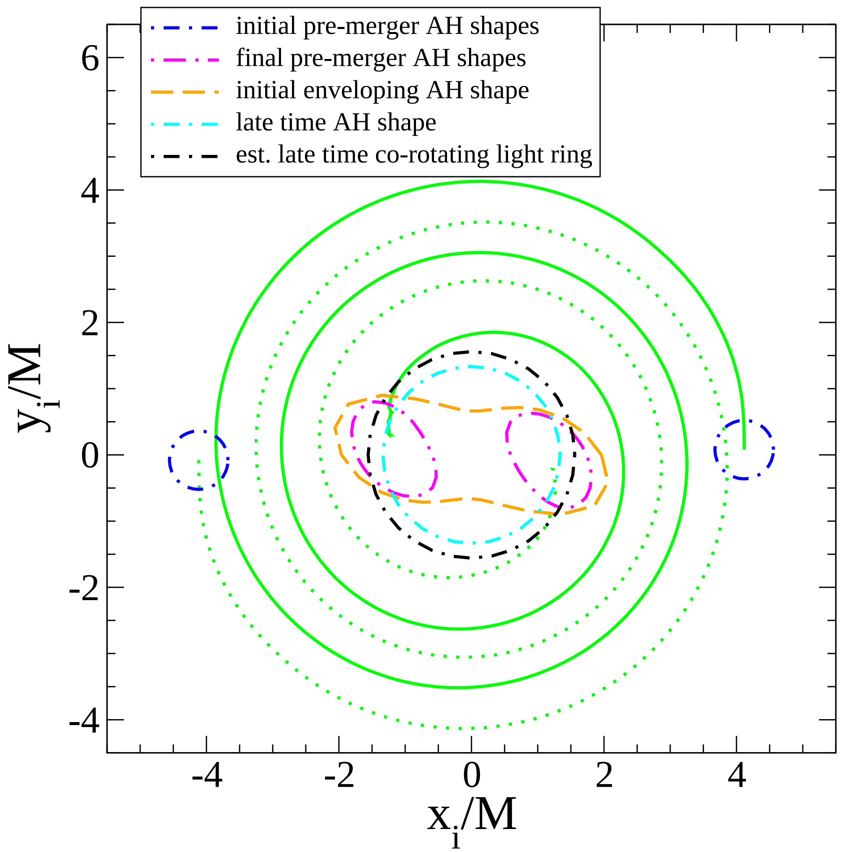

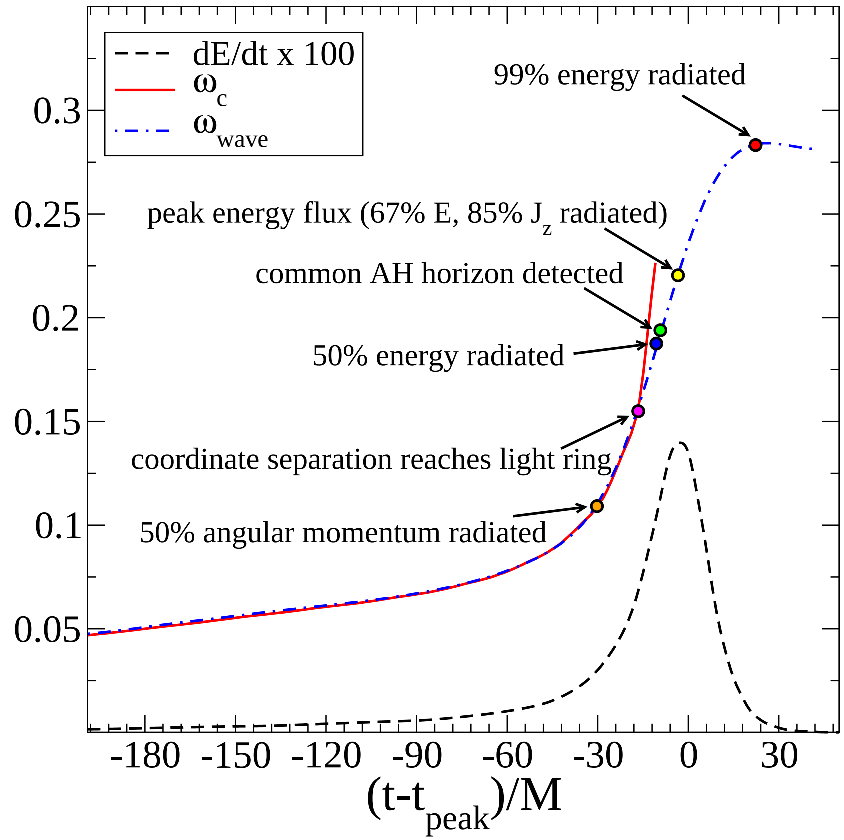

- *Short* **transition merger–ringdown**

[AB, Cook & Pretorius 06]

- **Energy and angular-momentum quickly released during merger**

Extremely accurate NR simulation using spectral methods

- **Equal-mass non-spinning black-hole binary** `Caltech-Cornell collaboration`

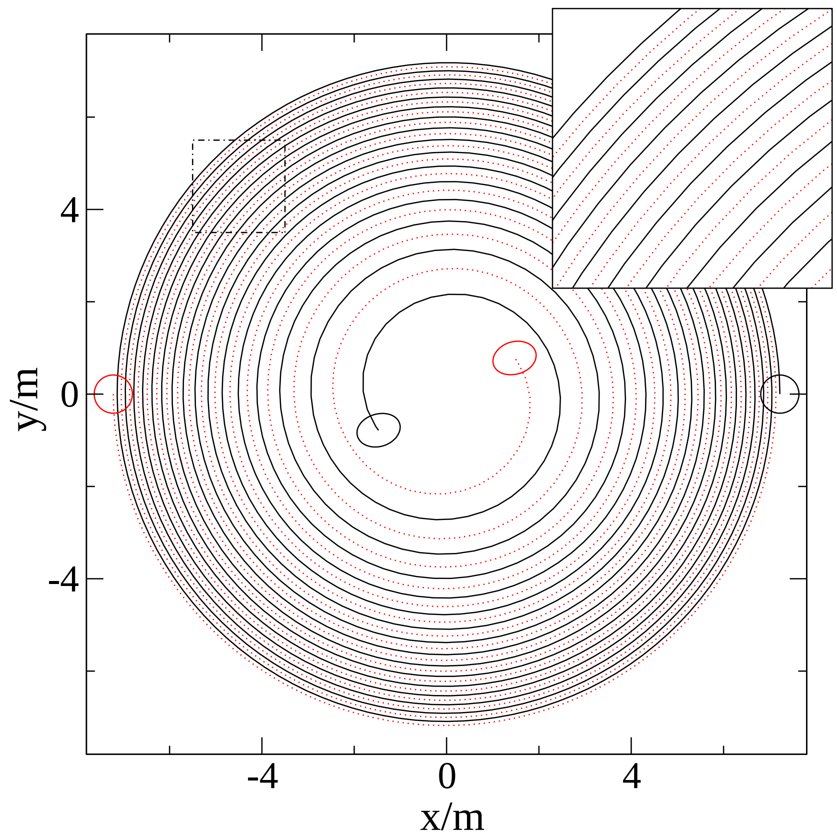

- **During the first 15 GW cycles all PN models agree with NR within 0.05 rad**

- **Different *adiabatic* PN models differ by the way we solve**:

$$\dot{\omega} = -\frac{F(\omega)}{[dE(\omega)/d\omega]}$$

Comparison between PN-expanded-approximants and extremely accurate numerical simulations (continued)

- **Equal-mass non-spinning black-hole binary** `Caltech-Cornell collaboration`
- **Later on the PN models accumulate a dephasing of few rads, except for one model**

[see also Nasa-Goddard 07; Jena 07]

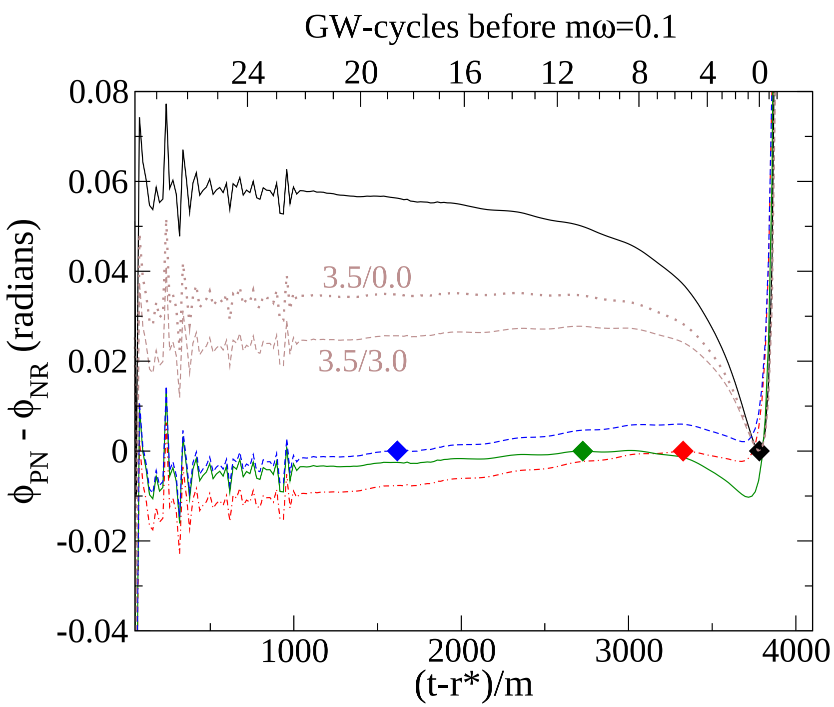

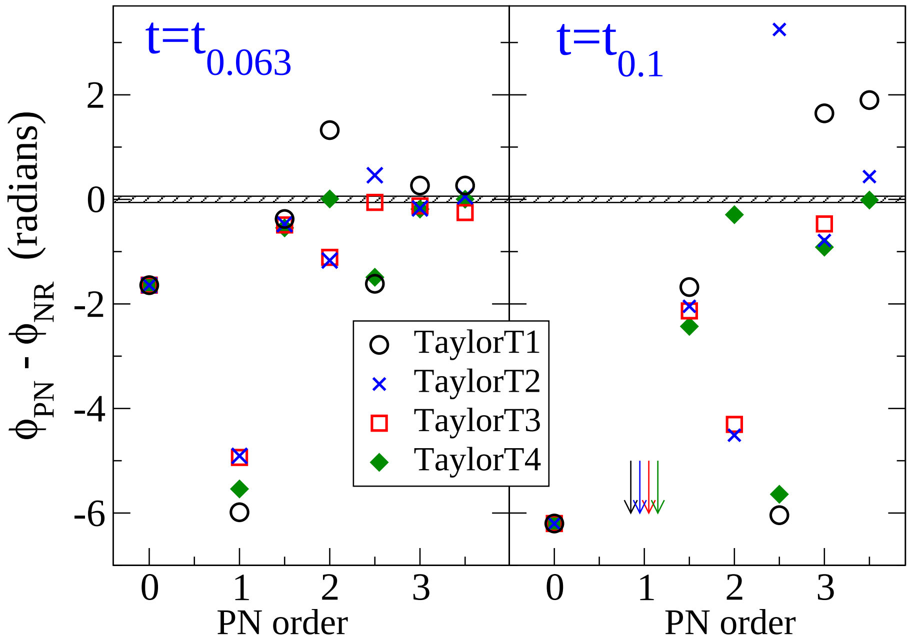

Comparison between PN-expanded-approximants and accurate numerical simulations

- **Equal-mass non-precessing, spinning black-hole binaries** [Hannam et al. 07]

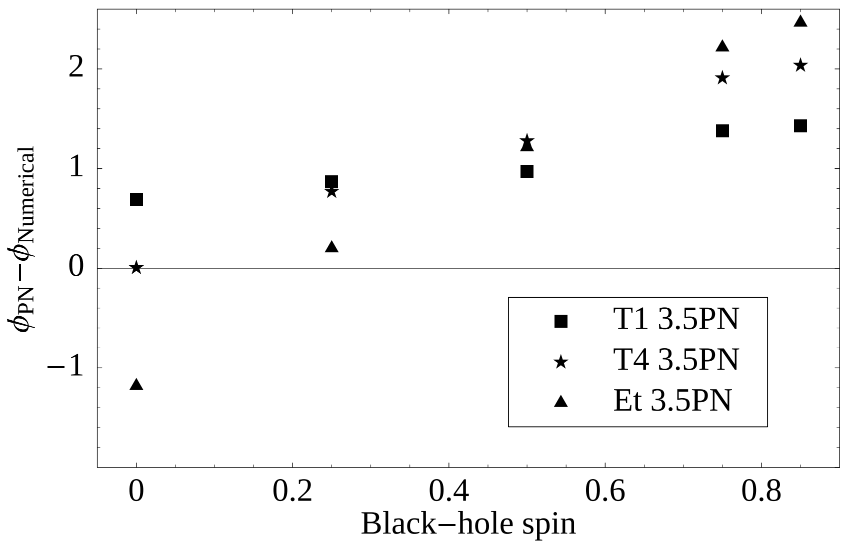

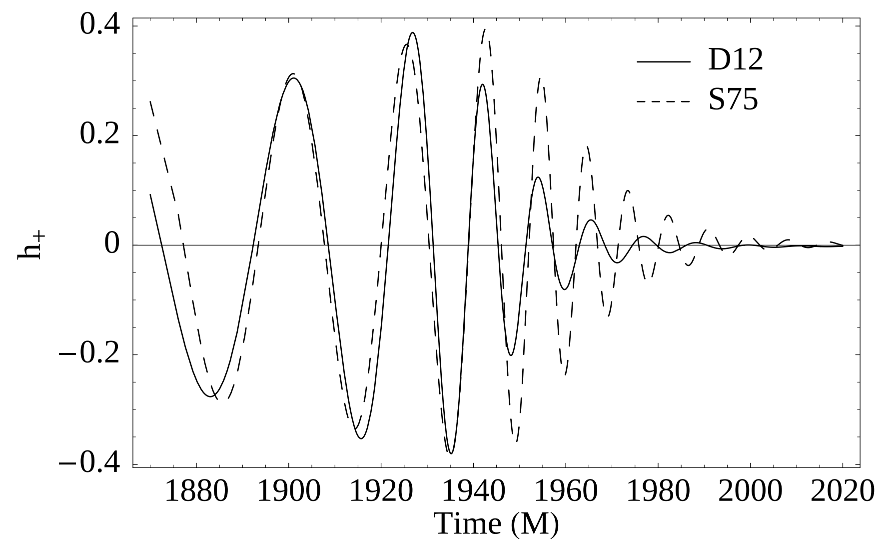

- **Higher-order spin corrections to the phase are needed**

[Will & Wiseman 96; Kidder 95; Blanchet, Buonanno, Faye 07; Faye, Blanchet & Buonanno 07]

[Port 06; Porto & Rothstein 06; Damour, Jaranowski and Schaefer 07]

Two separate issues

- **Less accurate templates (mild systematics) to** *detect the binary*

  $\Rightarrow$ *effectual* **templates**

- **Very accurate templates (low systematics) to** *extract binary parameters*

  different accuracy is required if testing astrophysics or general relativity

  $\Rightarrow$ *faithful* **templates**

  [Damour, Iyer & Sathyaprakash 98]

GW spectrum and frequency-domain templates

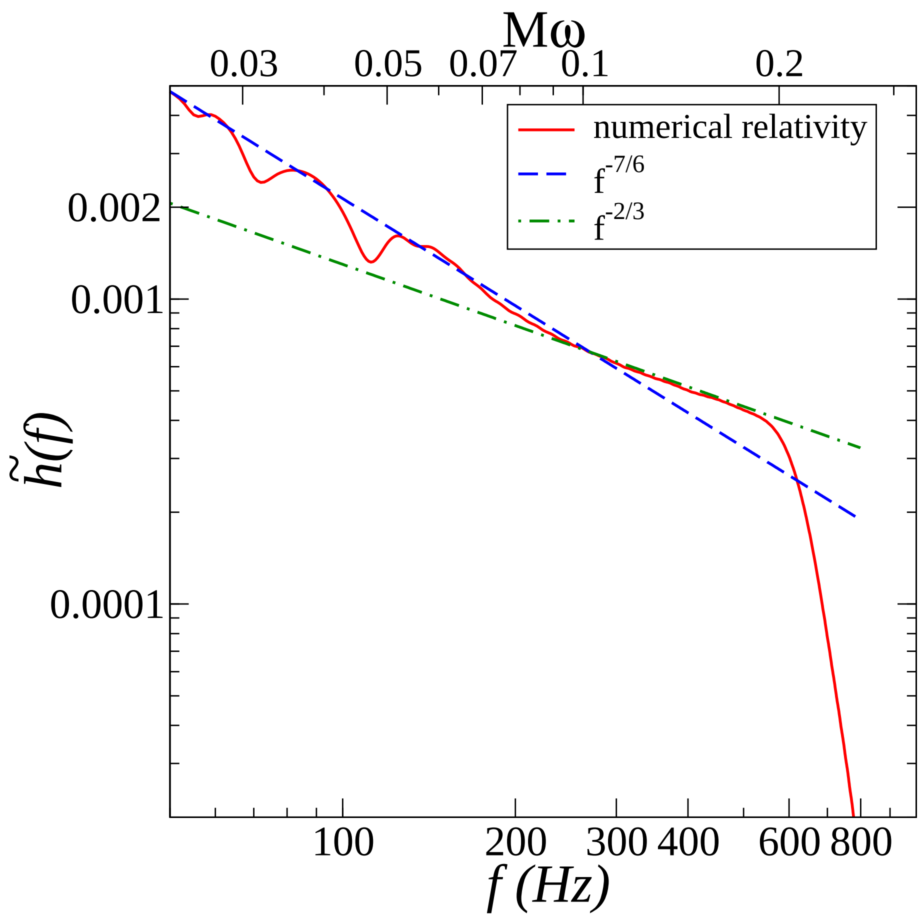

- $\widetilde{h}(f) = A(f)\, e^{i\,\psi(f)}\, \Theta(f_{\rm cut} - f)$

- $\psi(f) = 2\pi f t_0 - \phi_0 + \sum_{k=0}^{N} \alpha_k f^{k/3}$

- $f_{\rm cut} \simeq f_{220}^{\rm QNM}$

- **Instead of $f_{\rm cut}$, use change of *slope* and superposition of Lorentzians**

  [Ajith et al. 07; Pan et al. 07]

Change of slope: $f^{-7/6} \Rightarrow f^{\approx -2/3}$ [AB, Cook & Pretorius 06]

Comparing NR and SPA waveforms: *effectualness*

- Equal-mass case [Pan, AB, Pretorius & NASA-Goddard 07]

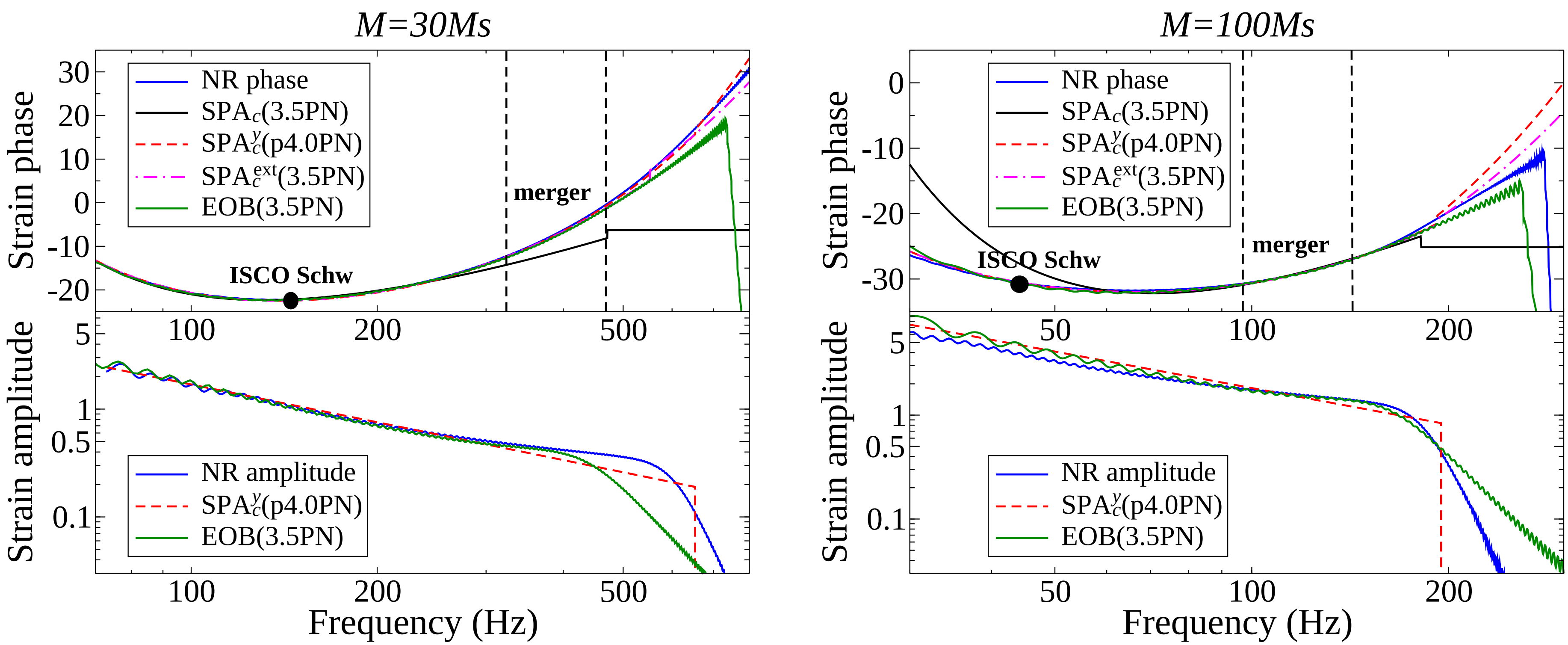

$$\psi_{\rm GW}^{\rm SPA}(f) = 2\pi f t_0 - \phi_0 - \frac{\pi}{4} + \frac{3}{128\eta v^5}\sum_{k=0}^{N}\alpha_k v^k$$ **with** $\alpha_8 = \mathcal{Y}\log v$ **and** $f_{\rm cut} \simeq f_{220}^{\rm QNM}$

Comparing NR and SPA waveforms: *effectualness* (continued)

[Pan, AB, Pretorius & NASA-Goddard 07]

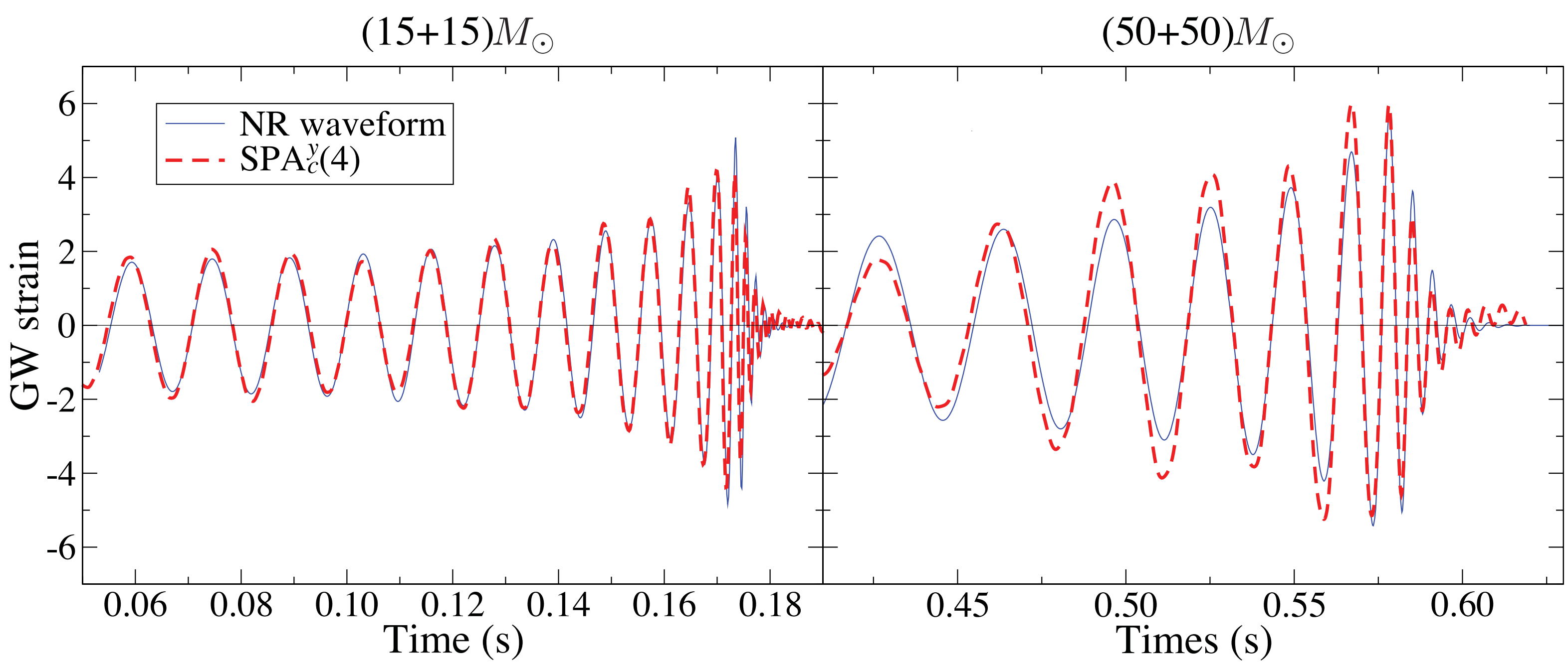

- **FF $\gtrsim$ 0.97 maximizing on binary parameters, time-of-arrival, initial phase**

Comparing NR and SPA waveforms: *effectualness* (continued)

[preliminary results by Pan using Caltech-Cornell waveform for non-spinning equal-mass binary]

- $M = 10 M_\odot$ **and LIGO spectral density: FF = 0.9735 between NR and SPA$_c$(3.5PN) maximizing on binary parameters, time-of-arrival, initial phase and** f_c **(**$f_c = 474$ **Hz). The template binary parameters are:** $M = 10.2054 M_\odot, \eta = 0.2342$

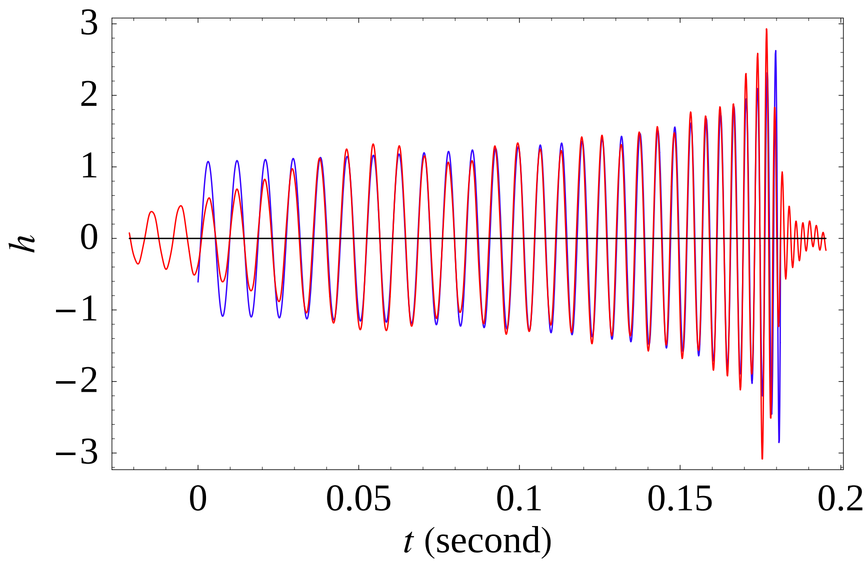

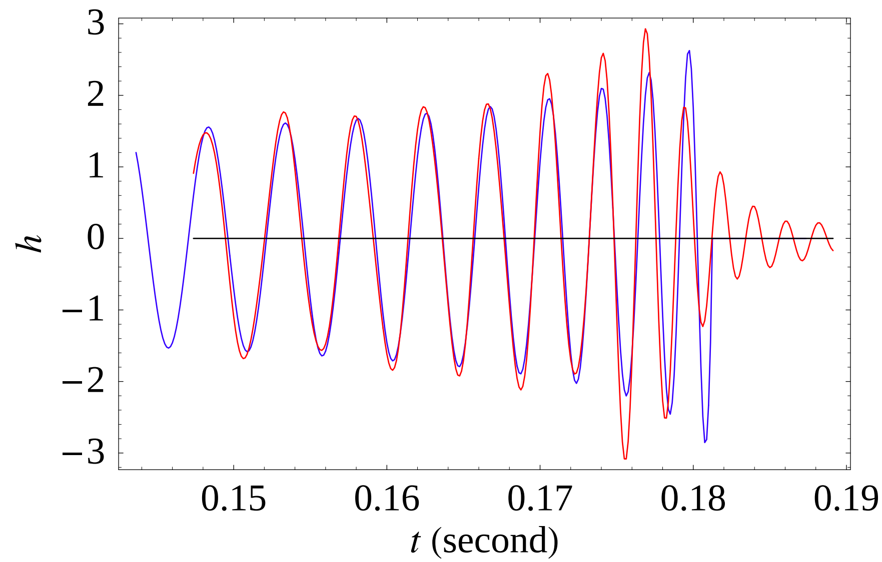

Phenomenological template bank in Fourier domain for merger-ringdown

[Ajith et al. 07]

$$A_{\rm eff}(f) \quad \equiv \quad C \begin{cases} \left(\frac{\pi M f}{a_0\eta^2+b_0\eta+c_0}\right)^{-7/6} & \text{if } f < \frac{a_0\eta^2+b_0\eta+c_0}{\pi M} \\ \left(\frac{\pi M f}{a_0\eta^2+b_0\eta+c_0}\right)^{-2/3} & \text{if } \frac{a_0\eta^2+b_0\eta+c_0}{\pi M} \leq f < \frac{a_1\eta^2+b_1\eta+c_1}{\pi M} \\ w\, \mathcal{L}\left(f, \frac{a_1\eta^2+b_1\eta+c_1}{\pi M}, \frac{a_2\eta^2+b_2\eta+c_2}{\pi M}\right) & \text{if } \frac{a_1\eta^2+b_1\eta+c_1}{\pi M} \leq f < \frac{a_3\eta^2+b_3\eta+c_3}{\pi M} \end{cases}$$

$$\Psi_{\rm eff}(f) = 2\pi f t_0 + \varphi_0 + \frac{1}{\eta} \sum_{k=0}^{7} (x_k\, \eta^2 + y_k\, \eta + z_k)\, (\pi M f)^{(k-5)/3}$$

Phenomenological template bank in Fourier domain: *faithfulness*

[Ajith et al. 07]

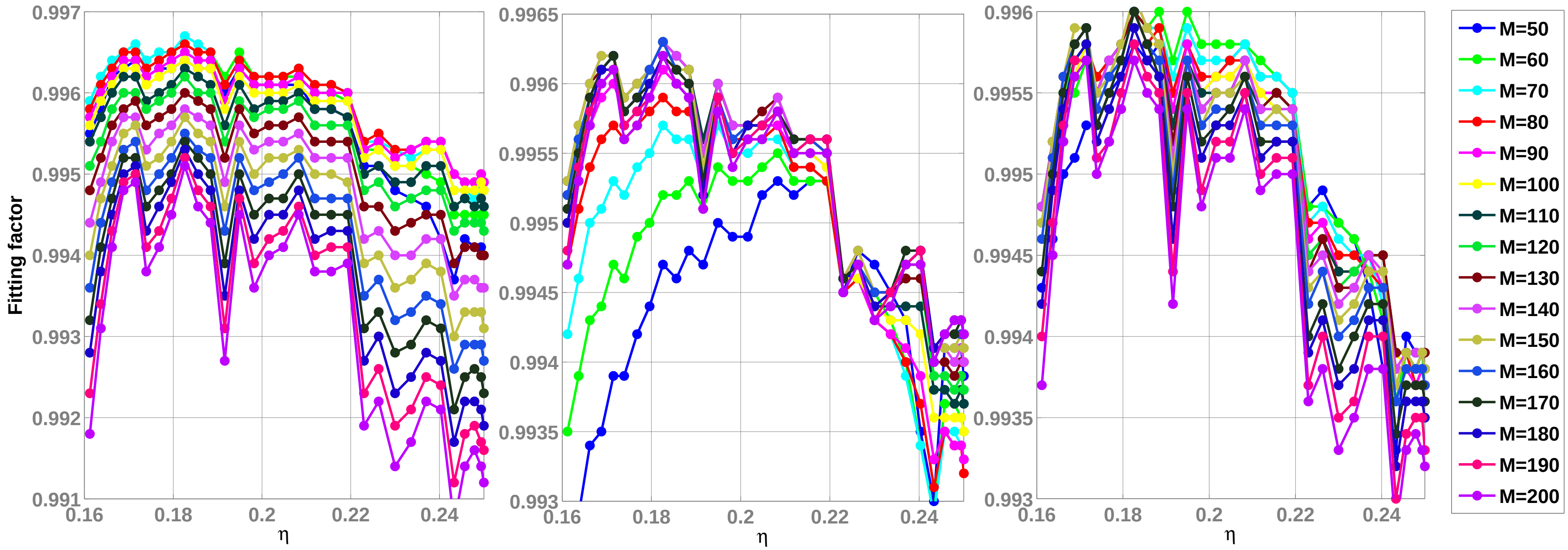

LIGO **Virgo** **Advanced LIGO**

Detectability for ground-based detectors

[AB, Cook & Pretorius 06; Baker et al. 06; Brady et al. 06; Pan, AB & NASA-Goddard 07]

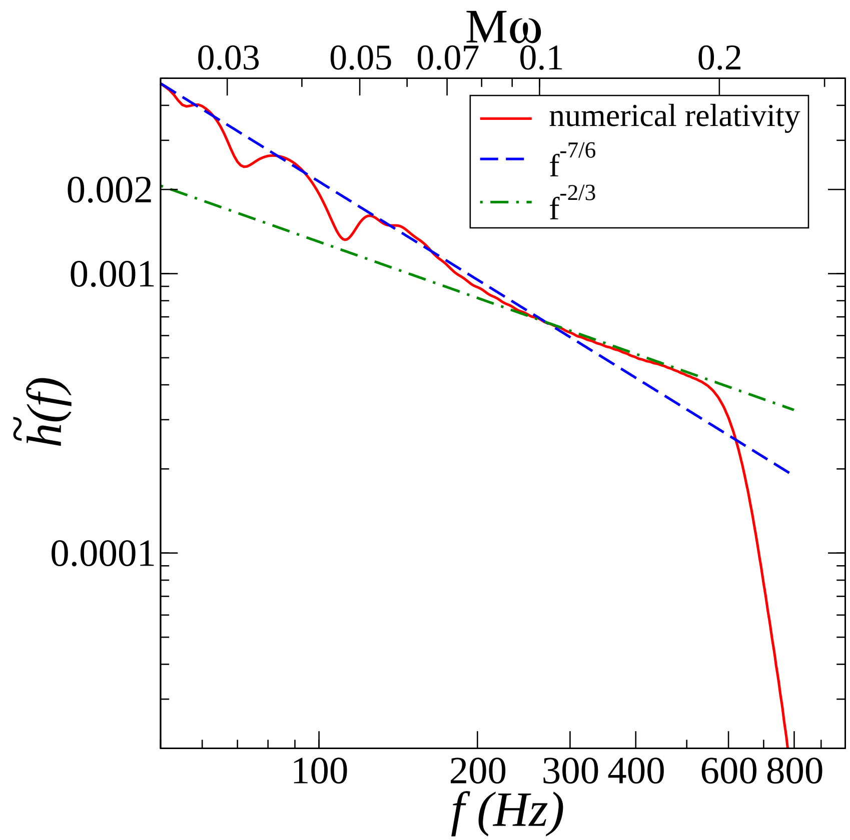

Change of slope: $f^{-7/6} \Rightarrow f^{\approx -2/3}$

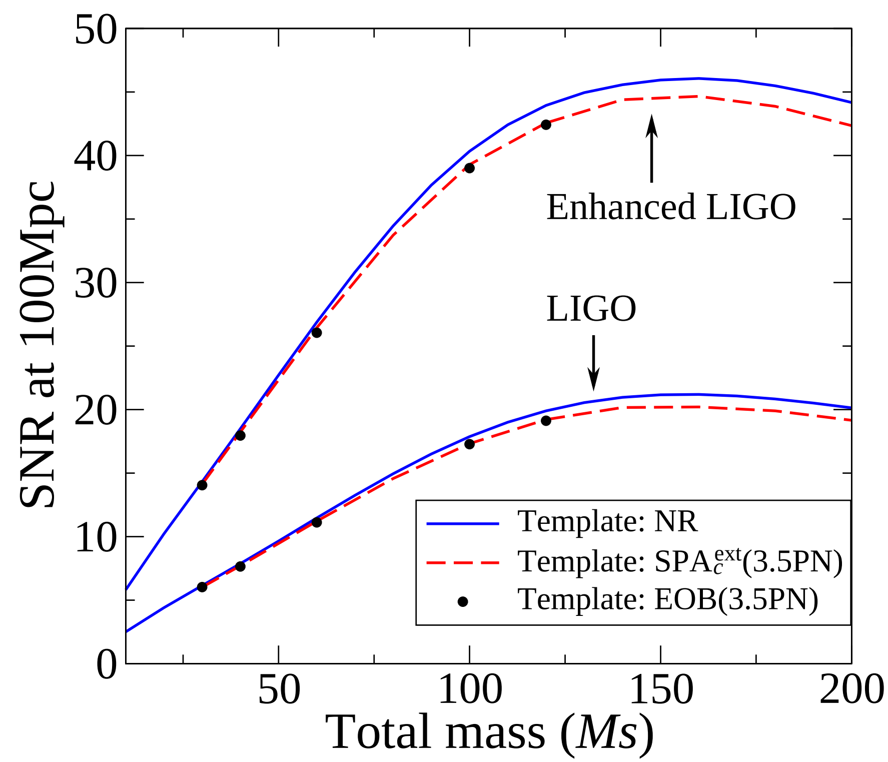

increase of SNR for $M > 40M_\odot$

Comparing NR and EOB waveforms: *effectualness*

[AB, Cook & Pretorius 06; see also Pan, AB & NASA-Goddard 07]

- **Fundamental QNM mode and two overtones included**

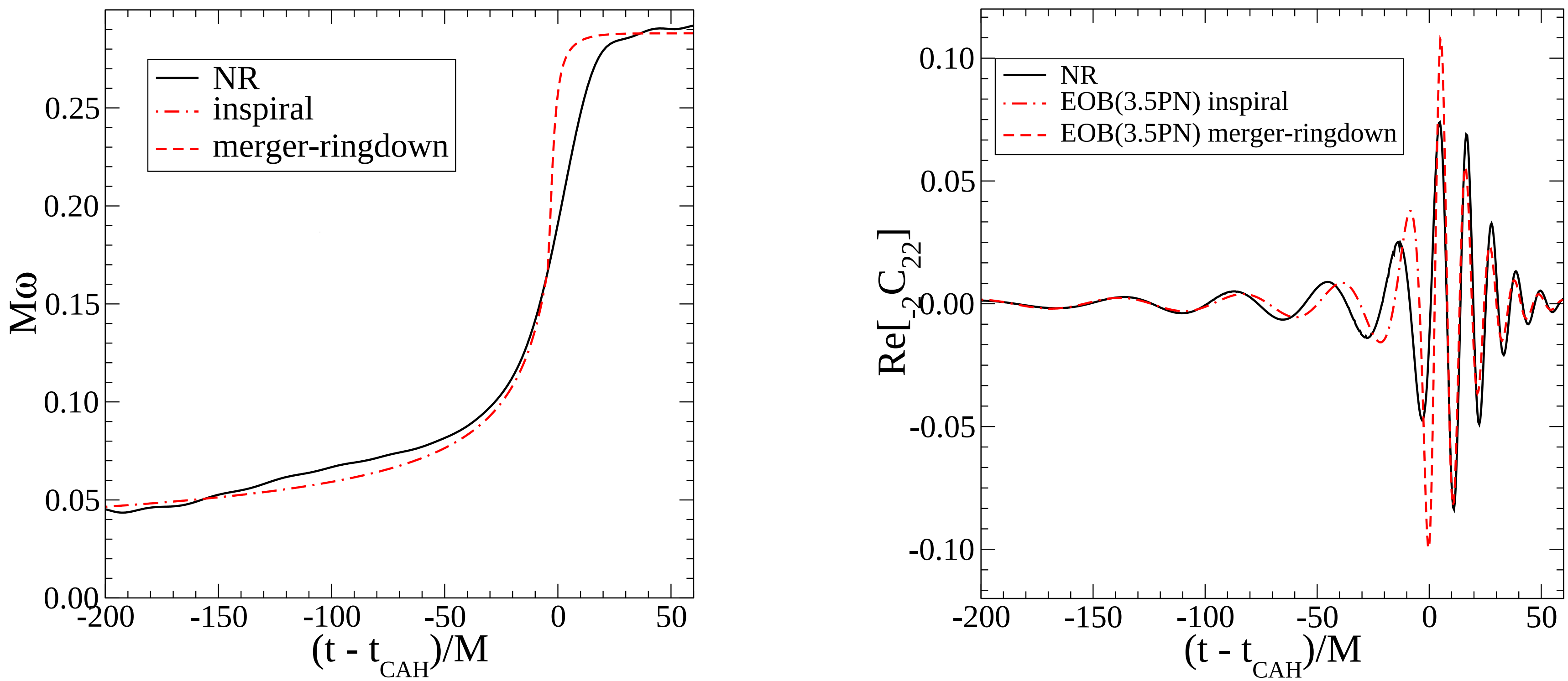

- **FF $\gtrsim$ 0.97 maximizing on binary parameters, time-of-arrival, initial phase**

Including ringdown modes in the EOB waveform

[AB & Damour 99; Damour & Gopakumar 06; AB, Cook & Pretorius 06; AB, Pan & NASA-Goddard 07; Schnittman, AB & NASA-Goddard 07; Damour & Nagar 07]

$$I^{\ell m}(t) = A(t)\, e^{-i\phi(t)} = \sum_{n=0}^{\infty} A_{\ell m n}\, e^{-i\sigma_{\ell m n}(t-t_{\rm match})}$$

The complex QNM frequencies $\sigma_{\ell mn}$ are functions of the final BH mass and spin. E. g., when matching three QNMs we solve for the complex amplitudes $A_{\ell mn}$:

$$\begin{pmatrix} 1 & 1 & 1 \\ -i\sigma_{\ell m0} & -i\sigma_{\ell m1} & -i\sigma_{\ell m2} \\ -\sigma^2_{\ell m0} & -\sigma^2_{\ell m1} & -\sigma^2_{\ell m2} \end{pmatrix} \begin{pmatrix} A_{\ell m0} \\ A_{\ell m1} \\ A_{\ell m2} \end{pmatrix} = \begin{pmatrix} I^{\ell m}(t_{\rm match}) \\ \dot{I}^{\ell m}(t_{\rm match}) \\ \ddot{I}^{\ell m}(t_{\rm match}) \end{pmatrix}$$

Improving EOB model using NR as *guide*

[AB, Pan & NASA-Goddard 07]

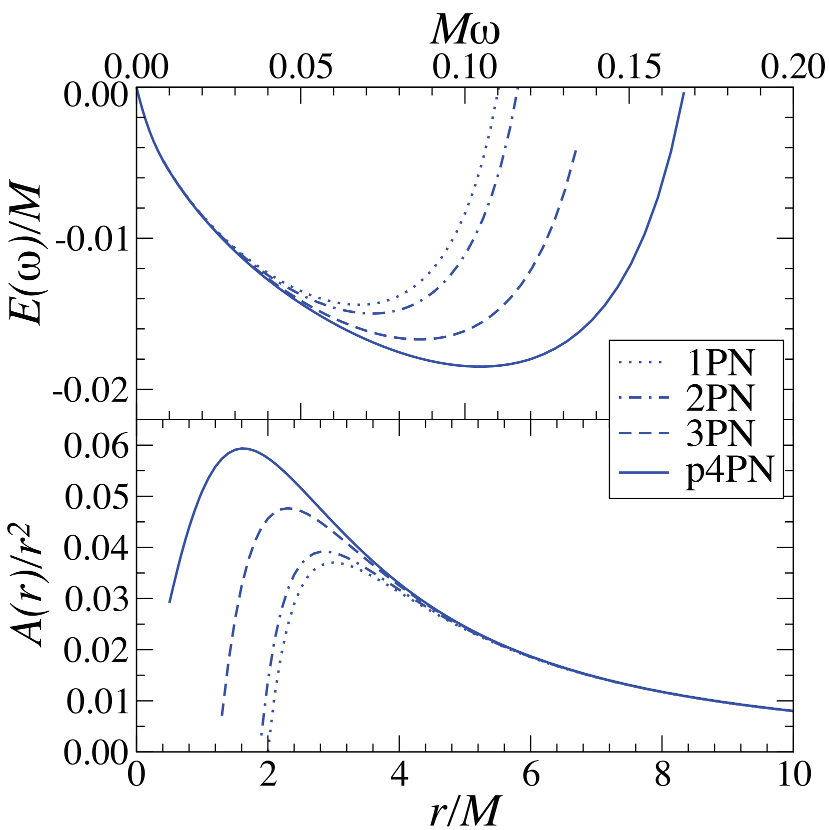

[Damour, Iyer, Jaranowski & Sathyaprakash 03]

- $A^{\rm p4PN}(r) = A^{\rm 3PN}(r) + \frac{a_5\,\eta}{r^5}, \; a_5 = 60$
- **Apply Padé resummation to ensure presence of LSO and light ring**
- **Analytic inspiral/ringdown matching point**

  $M\,\omega_{\rm match} = 0.133 + 0.183\,\eta + 0.161\eta^2$
- **QNM frequency and decay time depend** *only* **on** $M_{\rm BH}/M$ **and** $a_f/M_{\rm BH}$

  $$\frac{M_{\rm BH}}{M} = 1 + (\sqrt{8/9} - 1)\,\eta - 0.498\,\eta^2$$

  $$\frac{a_f}{M_{\rm BH}} = \sqrt{12}\,\eta - 2.90\,\eta^2$$

What determines the (non-adiabatic) frequency during the plunge?

[AB, Pan & NASA-Goddard 07]

- $\omega(t) = \frac{A(r)}{r^2}\,\frac{p_\varphi}{H^2}$

- $\omega_{\rm plunge}(t) \simeq \frac{A(r)}{r^2}\,{\rm const}$

$${\rm const} = \left[\frac{p_\varphi}{H^2}\right]_{\rm LSO}$$

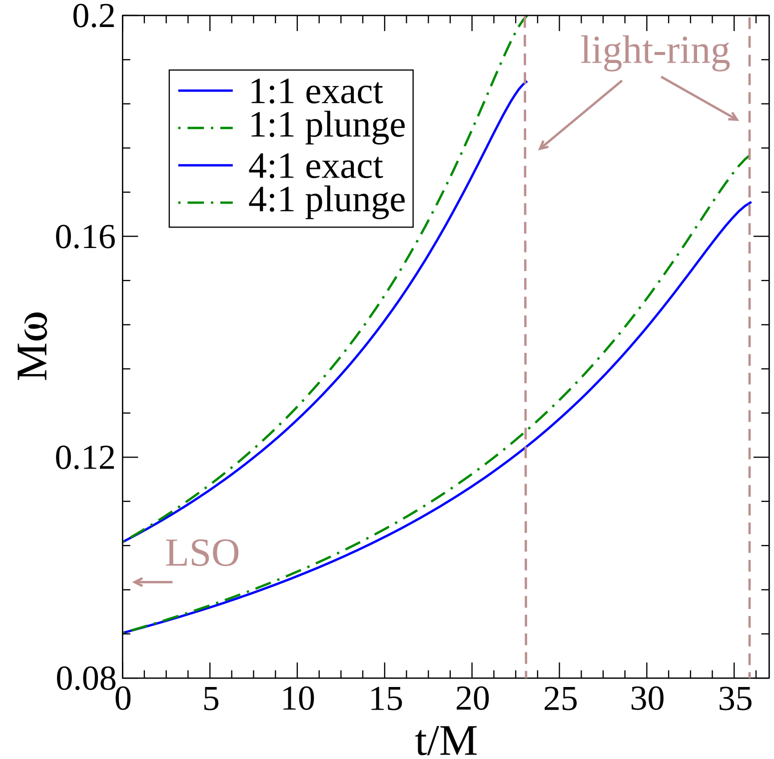

$\frac{A(r)}{r^2} \Rightarrow$ radial potential for a massless particle in Schwarzschild (light-ring)

NR and EOB waveforms for an equal-mass binary: *faithfulness*

- **Phase difference in GW cycles of** $\sim 5\%$ [AB, Pan & NASA-Goddard 07]
- **FF** $\gtrsim 0.98$ **maximizing** *only* **on time-of-arrival and initial phase**

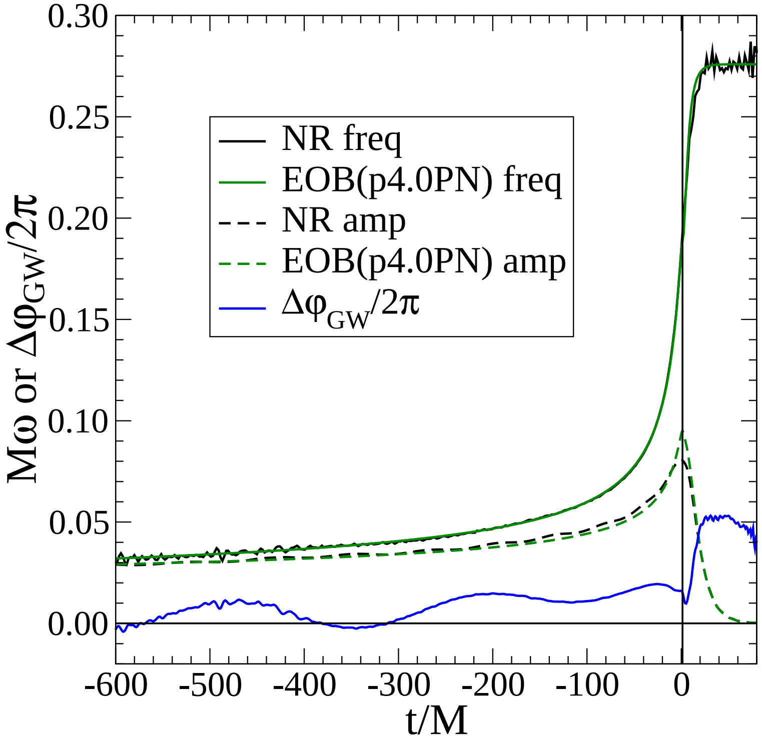

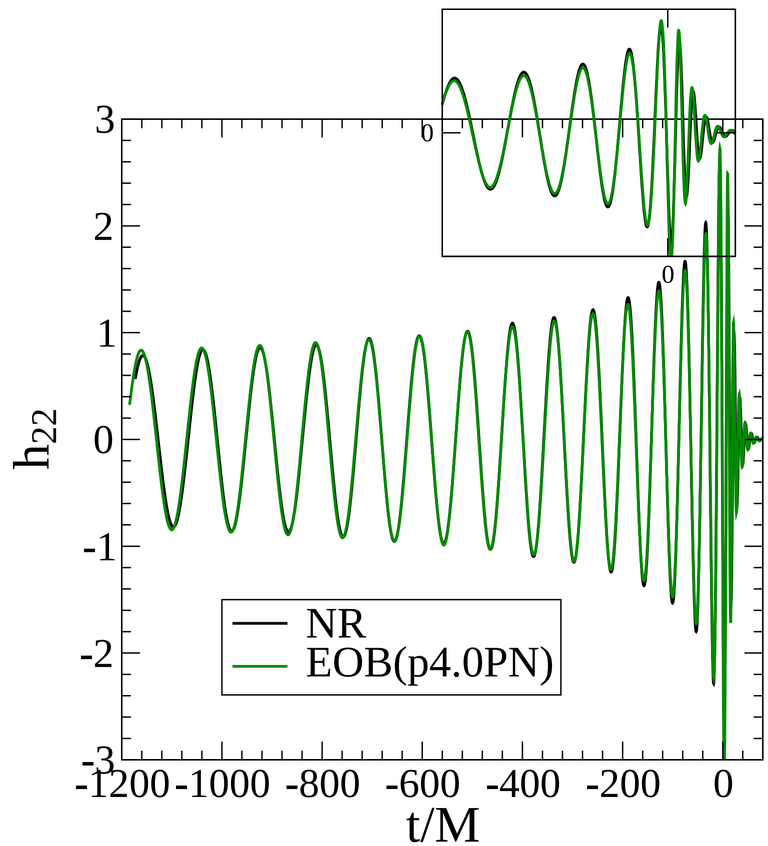

Unequal-mass binaries: several multipole moments

- **Mass ratio 4:1: modes with $l \neq 2$, $m \neq 2$ no longer sub-dominant**

[AB, Pan & NASA-Goddard 07]

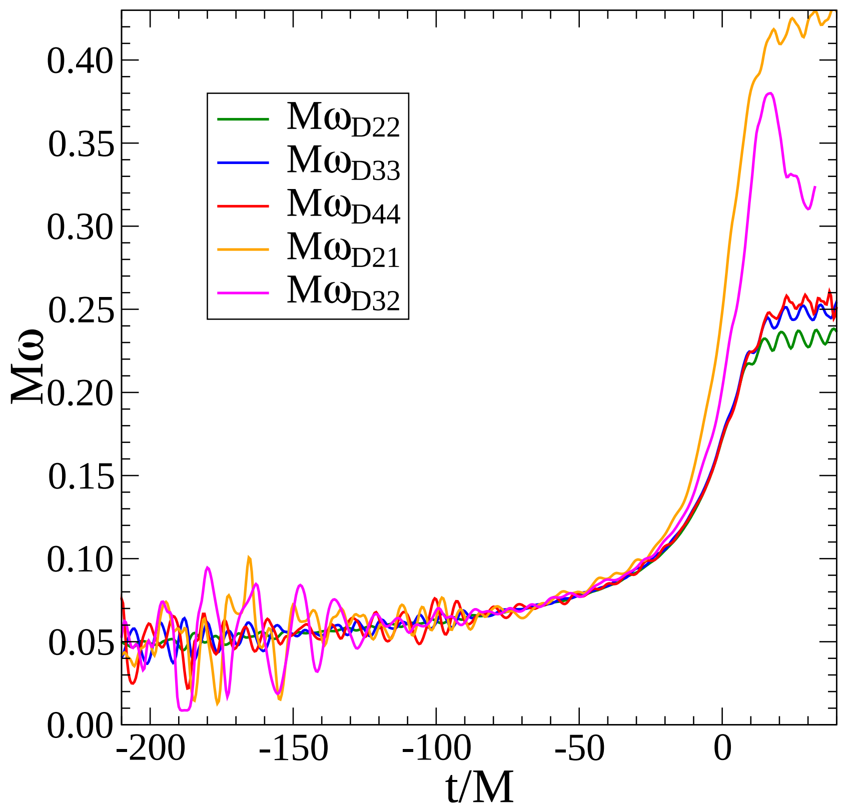

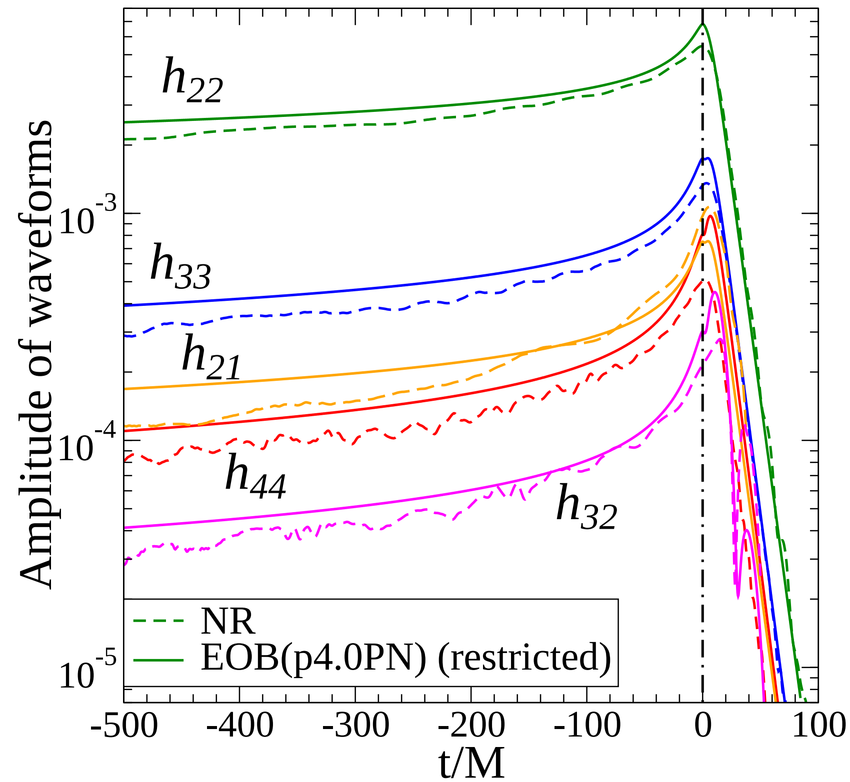

NR and EOB waveforms for an unequal-mass binary: *faithfulness*

- **Phase difference in GW cycles of** $\sim 8\%$ `[AB, Pan & NASA-Goddard 07]`
- **FF** $\gtrsim 0.98$ **maximizing** *only* **on time-of-arrival and initial phase**

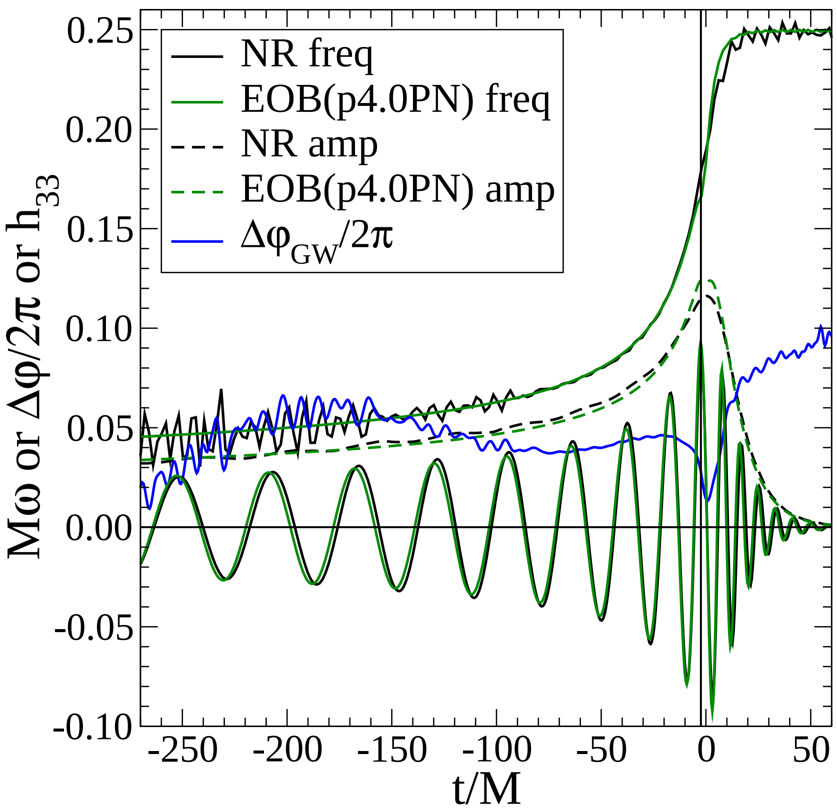

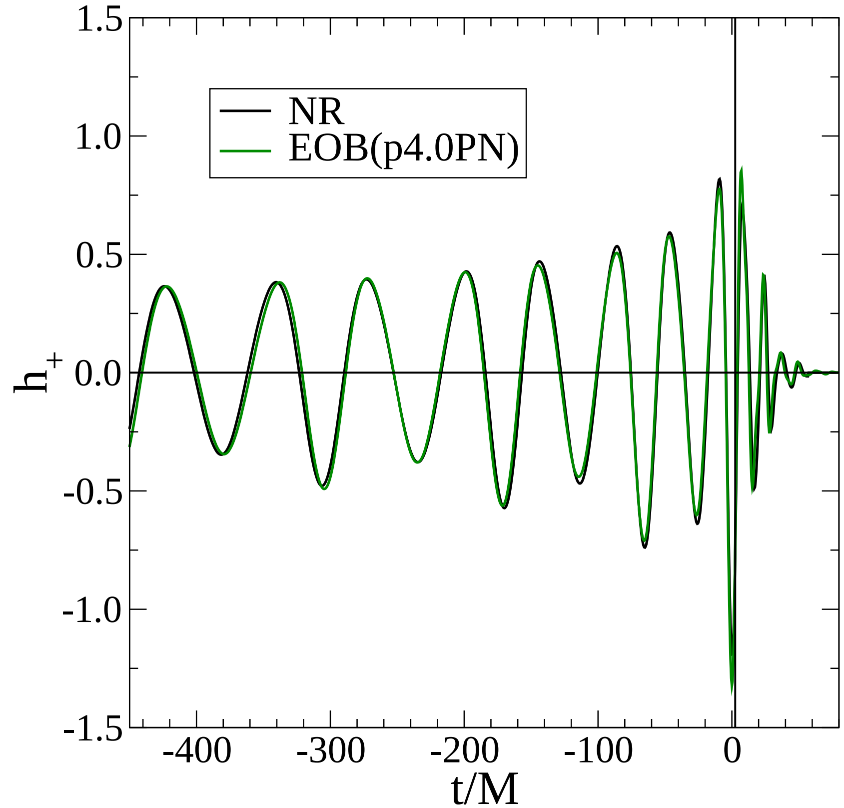

Suboptimal merger-ringdown match for subdominant modes

[AB, Pan & NASA-Goddard 07]

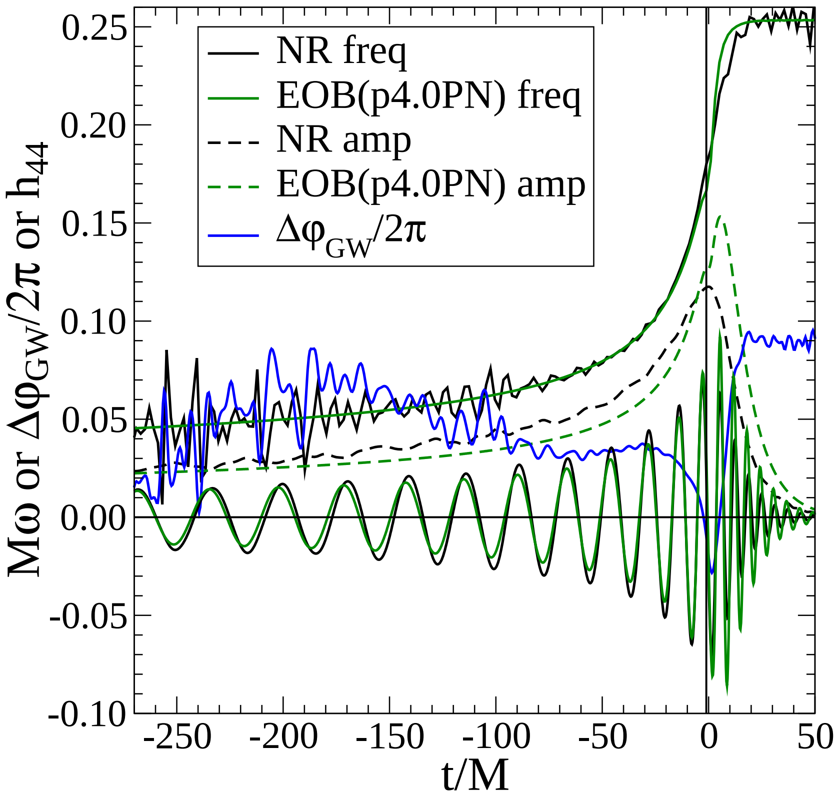

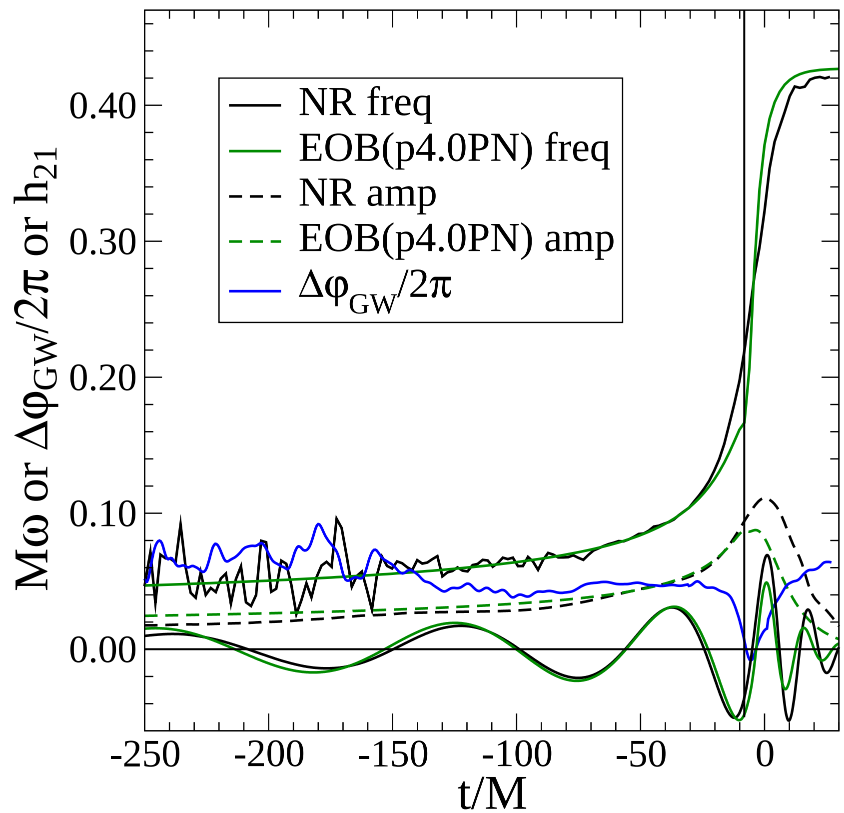

Comparison Regge-Wheeler-Zerilli and EOB in the test-mass limit

[Damour, Nagar & Tartaglia 06; Damour & Nagar 07]

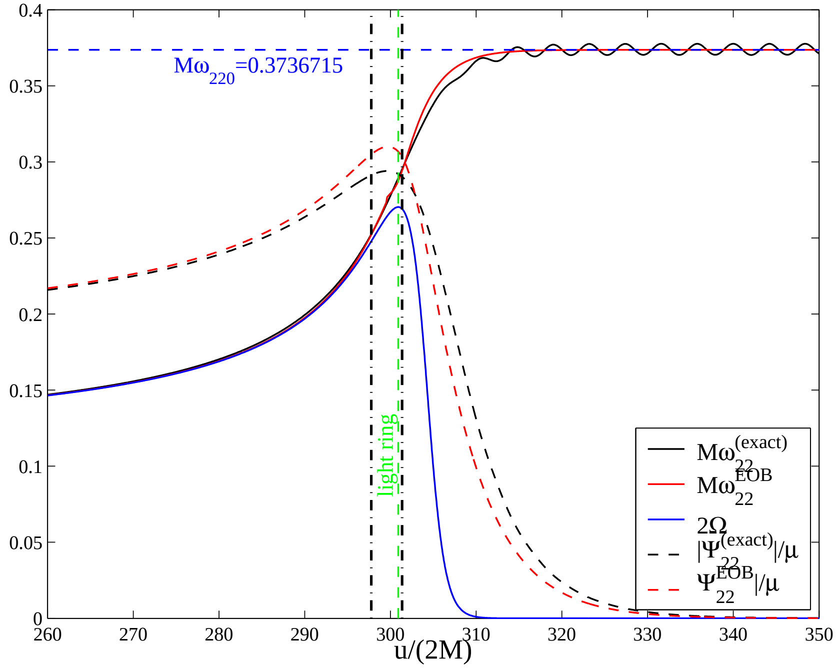

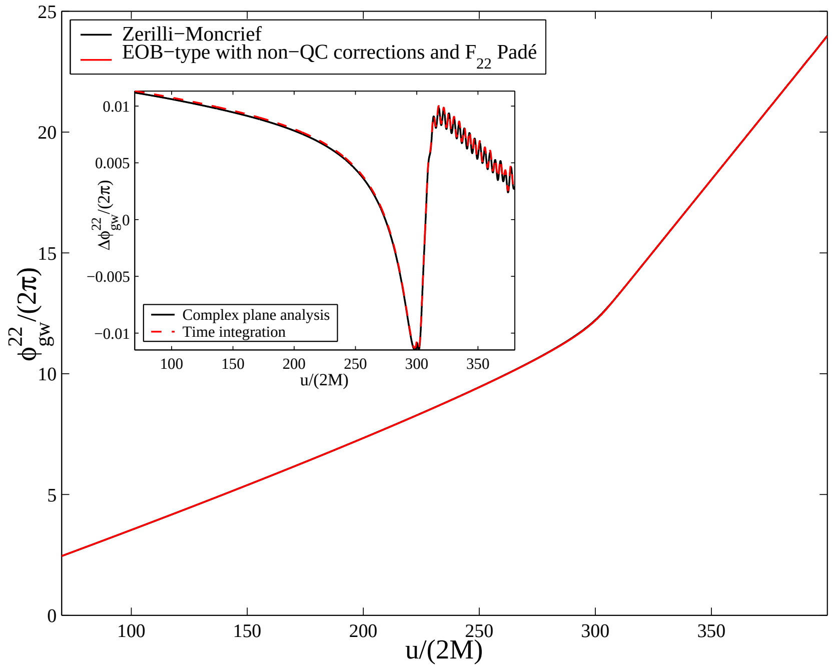

- **Several improvements: resummed higher-order amplitude corrections; deviations from quasi-circular motion; matching inspiral to ringdown on a *comb* instead of a point**

NR and EOB waveforms for an equal-mass binary: *faithfulness*

[Damour, Nagar & AEI-LSU 07]

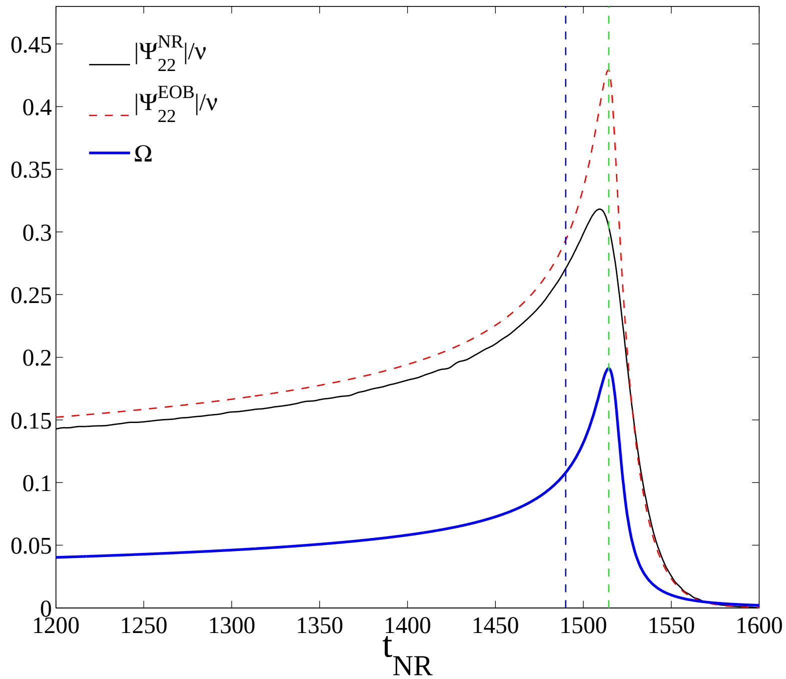

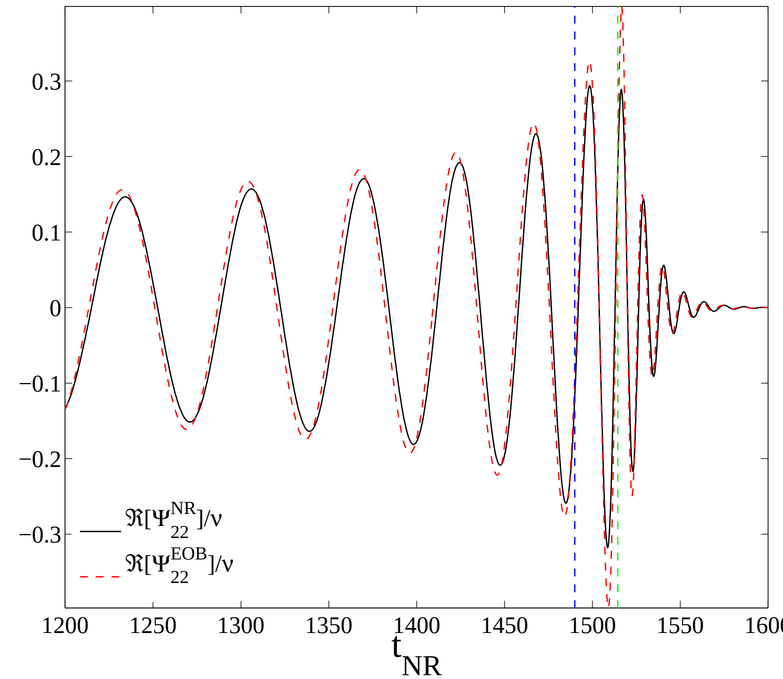

Using restricted waveform, $a_5 = 60$ **and the** *standard* $v_{\rm pole}$**.** $\Delta\varphi_{\rm GW}/2\pi = 0.023\%$

NR and further improved EOB waveforms for an equal-mass binary: *faithfulness*

[Damour, Nagar & AEI-LSU 07]

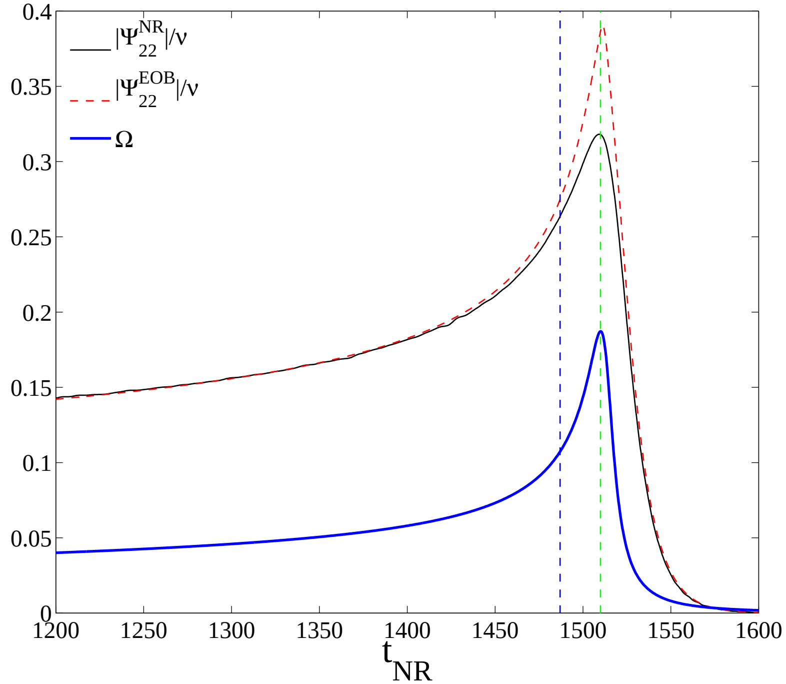

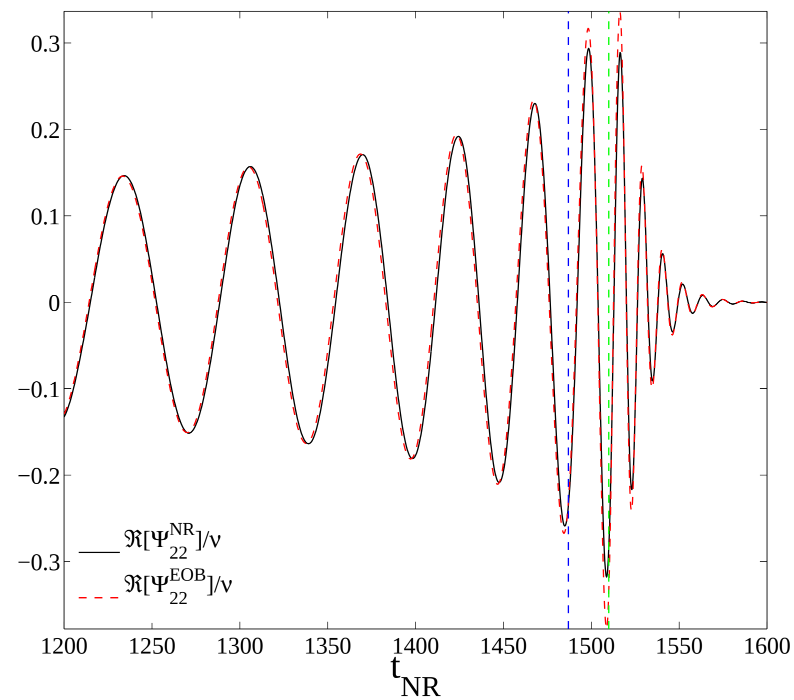

Using resummed ampl., $a_5 = 60$ **and** $v_{\rm pole} = 0.536$**, , comb, etc.** $\Delta\varphi_{\rm GW}/2\pi = 0.01\%$

Comparison between EOB and an extremely accurate numerical simulation

- **Equal-mass non-spinning black-hole binary** `[Caltech-Cornell collaboration]`

`[Damour & Nagar 07]`

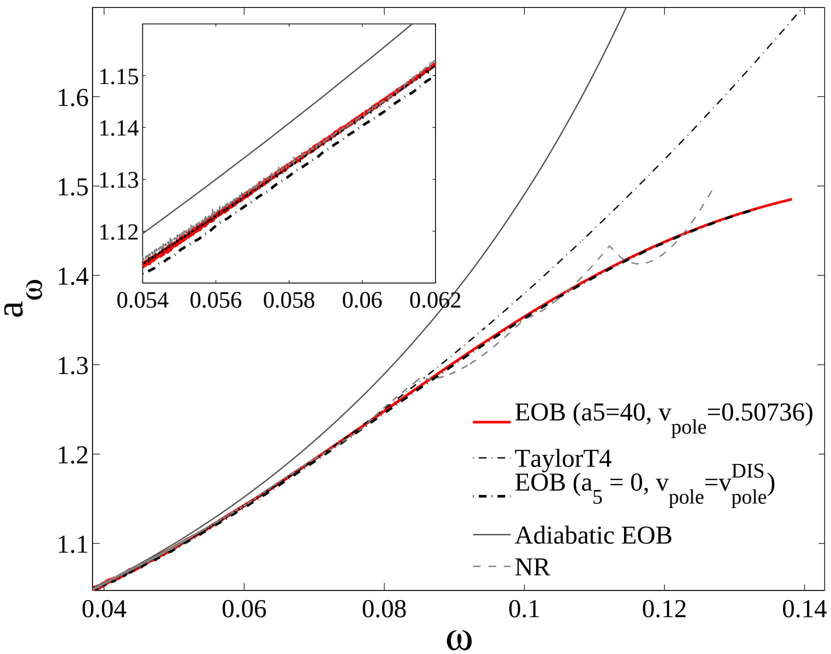

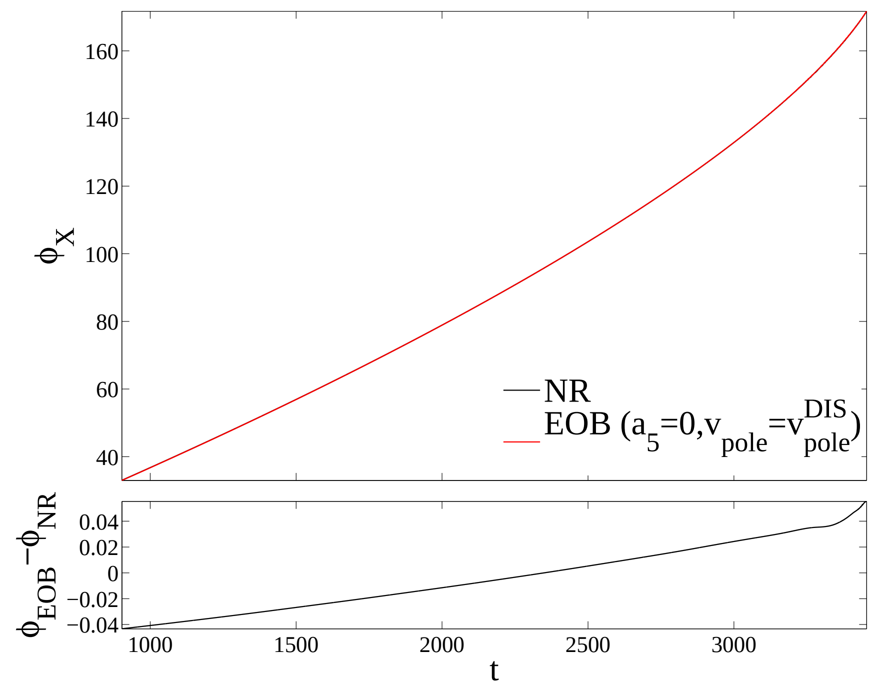

Comparison between EOB and an extremely accurate numerical simulation

- **Equal-mass non-spinning black-hole binary** `[Caltech-Cornell collaboration]`

[preliminary results Caltech-Cornell/Maryland]

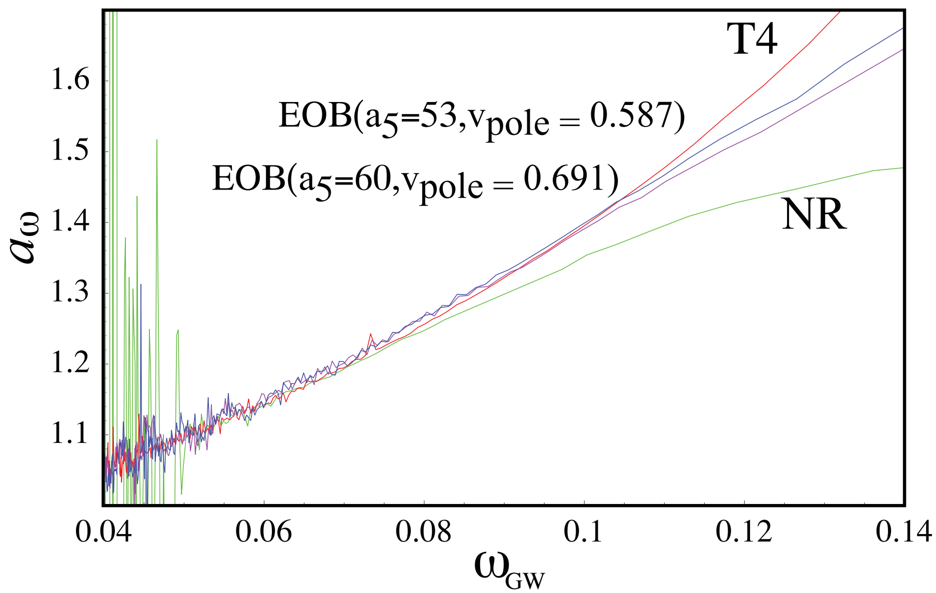

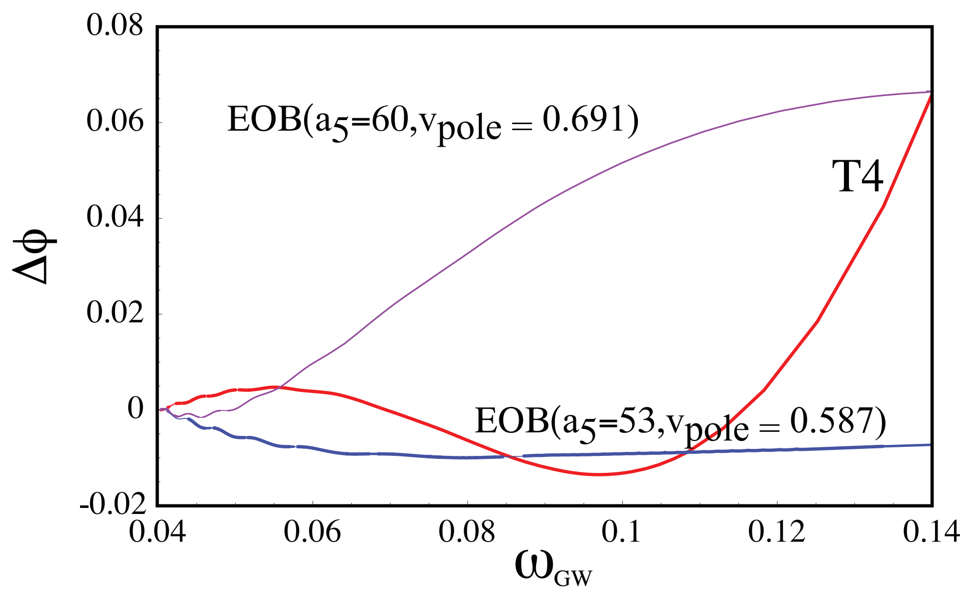

- **Other adjustments might be needed when merger-ringdown is included, and when different mass ratios are considered**

The spin and mass of the final black hole

[Berti et al. 07; Damour & Nagar 07; AB et al. 07; Boyle et al. 07; Sperhake et al. 07; Rezzolla et al. 08]

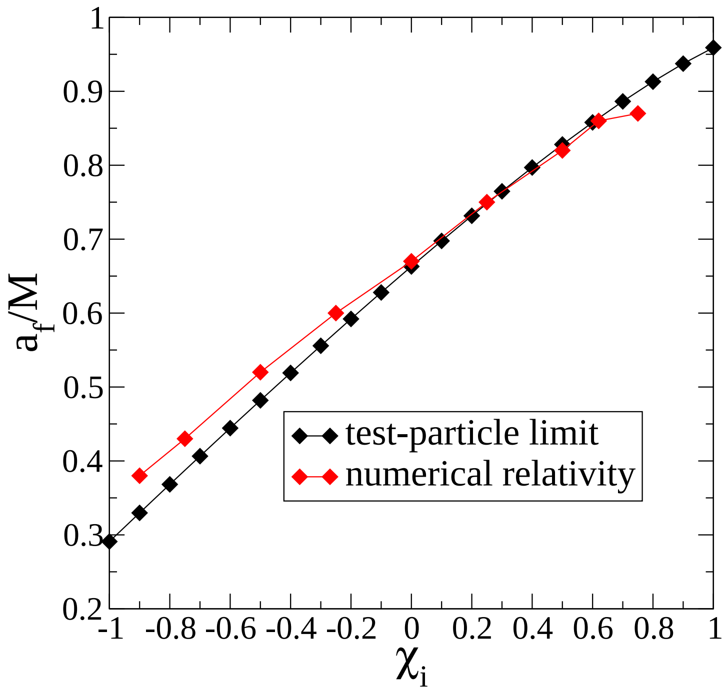

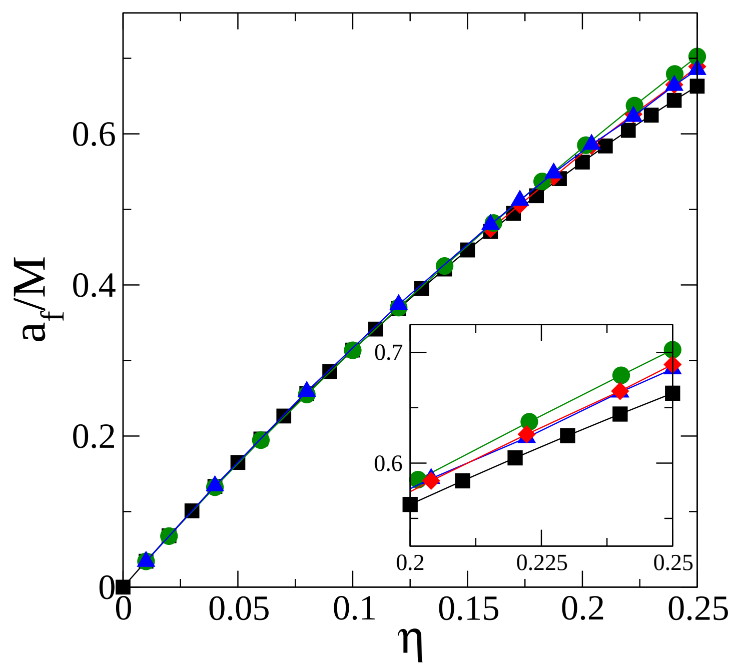

$$\frac{a_f}{M} = \frac{L_{\rm orb}^{\rm ISCO}(a_f,\eta)}{M^2} + \frac{S_1}{M^2} + \frac{S_2}{M^2} \Leftarrow$$ **using Kerr spacetime** [AB, Kidder & Lehner 07]

Summary

- *Simplicity* of (non-spinning) binary coalescence waveforms is helping in modeling analytical templates
- Several similarities with the test-mass limit case
- EOB/Padé resummations can condense the dynamics in a few functions $\Rightarrow$ natural flexibility to be employed for building an analytic model for the full waveform
- The EOB waveforms calibrated to the numerical-relativity results can achieve very high matching performances all along inspiral, merger and ringdown
- Phenomenological and physical template families in the Fourier domain can also perform rather well either for the inspiral or merger-ringdown
- So far, only a small region of the parameter space has been explored. The comparisons should be extended to much longer and accurate spinning, precessing binary simulations and should include all relevant gravitational modes